1

INTRODUCTION

1.1 AIR POLLUTANTS

Air pollutants are known as a substance in air, in such quantities and of such duration liable to cause harm to human and the environment. Air pollutants can be found everywhere- indoor or outdoor, and it can be in the form of solid particles, liquid droplets or gasses. The largest amount of air pollutants originated from human activities, although there are some natural causes as well, such as volcanic eruptions.

Air pollution has the following effects:

(a) Atmospheric effects, which may include changes in: (1) visibility, (2) climate, (3) frequency of rainfalls, (4) precipitation chemistry, and (5) stratospheric ozone levels.

(b) Health effects: which may be direct (e.g., pollutants come in contact with eyes) or indirect (e.g., pollutants enter the blood stream from lungs).

(c) Welfare effects: which may include damages to vegetation, livestock or even materials.

When pollutants are first released from a source, their concentrations are usually high, and effects on environmental quality may be immediate. Dispersion must take place quickly in a limited portion of the atmosphere. Initially, dispersion is influenced by microscale (e.g., plume behavior, currents, etc.), mesoscale (e.g., sea breeze, valley winds, etc.) air motions, and then by cyclones and anticyclones of macroscale motion (Godish, 1991). As dispersion processes dilute pollutants, they may undergo chemical and physical transformation before depositing in rain or snow (wet deposition) or as dry

gas or particles (dry deposition). The deposition processes cause pollution of land, freshwater or the seas, according to where they occur.

1.2 AIR PARTICULATE

Airborne particles are tiny subdivisions of solid or liquid matter suspended in a gas or liquid, forming atmospheric impurities. A suspension of airborne particles, whether liquid droplets or solids, is generally referred to as an aerosol. Typically, aerosols are composed of particles of many different sizes. Different aerosols have different degrees of size dispersion. Particles smaller than about 10 μm in diameter are able to remain airborne for hours or days, and, in some cases, even weeks, and it is this range of particle sizes with which air pollution science is most normally concerned. Particles greater than around 10 μm in diameter are large enough to settle quite quickly from the atmosphere under the influence of gravity and can cause nuisance through their ability to deposit out on horizontal surfaces, creating dust soiling, whilst the smaller particles are most notable for the health hazard which they present (Harrison, 2004). Suspected adverse health effects on even low levels of airborne particulate matter have led to increase concern over how fine particulate concentrations might best be controlled. (Dockery *et al*., 1993).

Particles are often classified by their aerodynamic properties because (a) these properties control the transport and removal of particles from the air; (b) they also control their deposition within the respiratory system; and (c) they are associated with the chemical composition and sources of particles. The chemical composition of fine particulate matter is extensively controlled by emissions from terrestrial, marine and various anthropogenic sources.

The study of chemical composition of air particulate matter is of major importance for several reasons: anthropogenic compounds and some of their atmospheric transformation products present in atmospheric aerosols often represent a high potential hazard to human health (Bayona *et al*., 1994). Atmospheric aerosols are of climatic importance due to their optical properties to absorb and scatter solar radiation depending on their chemical composition. They also affect tropospheric chemistry and in particular ozone and nitrogen oxide budgets because relevant heterogeneous reactions occur on their surface. Last but not least, the atmosphere constitutes a conveyor belt for naturally emitted compounds and anthropogenic chemicals to the ocean (Prahl *et al*., 1984; Gagosian and Peltzer, 1986; Fernandez *et al*., 1992)

Different names are being used for different types or fractions of air particles. The organic fraction is formed by a mixture of compounds, including aliphatics, aromatics, aldehydes, ketones, alcohols, acids and nitrates, whose nature is still scarcely known.

1.3 ORGANIC AIR PARTICULATE MATTER

Organic matter and its lipid components are naturally occurring materials, but their composition may be influenced by many human activities. Organic components of the atmosphere in gas as well as condensed phase in polar regions have recently gained a great concern in the frame of the earth sciences, environmental protection and global change studies (Barrie *et al*., 1992; Muir *et al*., 1992; Thomas *et al*., 1992). Organic aerosol pollution has always been an interest of scientists because of the potential detrimental human health effects (e.g., asthma, emphysema) with the associated toxic organic compounds (Abelson, 1998; Oanh *et al*., 2002).

The composition of aerosol particles depends on their sources. Some particles occur naturally, originating from volcanoes, dust storms, forest and grassland fires, living vegetation, and sea spray. Human activities, such as the burning of fossil fuels in vehicles, power plants and various industrial processes also generate significant amounts of aerosols. Biogenic organic matter, consisting predominantly of lipids, soot and humic, and fulvic acids, is now firmly established as a major carbonaceous fraction in atmospheric particles (Eichman *et al*., 1979; Simoneit *et al*., 1980; Simoneit and Mazurek, 1982).

Since organic air particulate matters have become a subject of concern, some research has been undertaken on the origin, constitution, transport, fate, and effects of the particulate components. Many investigations have been carried out on airborne organic matter, most of them with the aim of measuring organic pollutants in urban, suburban and rural areas. Much fewer studies have focused on characterization of the organic matter over the ocean.

1.3.1 Marine Aerosols

Marine coastal areas are subject to a great deal of stress from human activities as modern civilization spreads, as more than half of the world population now lives within 200 km of the coast and that number is still increasing (De Souza *et al*., 2003). Abundant natural and anthropogenic organic matter derived from land and carried by rivers and the atmosphere are imported to and buried in marine coastal areas (Gao *et al.*, 2008). Besides that, the ocean itself contains vast number of organisms and microorganisms that undergo many processes. This contributes to the amount of organic matter found within the marine and coastal environment. Earlier reports on organic components of atmospheric particulate matter over the oceans describes mainly lipids characteristic of higher plant waxes from continental sources and minor marine derived

lipids from plankton and microbial detritus (Simoneit 1977, 1980; Marty and Saliot, 1982; Simoneit *et al*., 1991a).

1.4 SAMPLING AND SAMPLE PRETREATMENT

1.4.1 Sampling and sampling artifacts

Sampling is the most critical step within the total scheme of atmospheric analysis. Because of the arbitrary and complex dynamic nature of air, in terms of temporal and spatial fluctuations of gaseous and particulate analytes, many sampling problems still exist (Niessner, 1993). The collection of air particulate matter for organic analysis is done by a variety of technique; the classic technique is high-volume air sampler using standard glass fiber filters.

High volume sampling is necessary to collect enough material for a detailed organic speciation. No special devices, such as denuders for pre-removal of gaseous oxidants and VOCs, and foam plugs for post-filter collection of volatilized particulate components from the filters were used because of the experimental difficulties in applying such devices to high volume sampling (Pio *et al*., 2001).

Cincinelli *et al*. (2001) carried out the aerosols sampling with a 5-stage cascade impactor, located at the top of high volume air sampler, which separated atmospheric particles into six different size fractions. Air sampler were connected to computerized meteorological system which will activate the sampler device only under well-defined weather condition: absence of rain, winds from the sea in a sector between 1858 and 2258 and wind speed >10 m/s. Sampling started when all these conditions were constant for at least 30 min. Pio *et al*. (1996) used single stage impactor plate to separate particles into two size fractions, with high volume air sampler at the flow rate of 1.13

m^3/min. Aerosol samples was collected on pre-treated and washed Whatman QM-A quartz fibre filters (Pio *et al.*, 1991).

Cecinato et al. (2000) collected the air particulate samples onto 0.47 mm Teflon fibre (previously cleaned by heating up to 50 °C for a night). A medium volume sampling device was used, suitable for the selective collection of the pulmonary fraction particulates (i.e. particles ranging from 0.01 to 10.2l mm in diameters). It was equipped with a flow rate controller and was set at 1 m^3/h. When the sampling was completed, filters were weighed, wrapped in proper envelopes, sealed and stored in the dark at cool temperature (4 °C) until analysis.

Schauer *et al.* (1996) uses four parallel 47 mm diameter filter assemblies containing three different types of filters: two quartz fiber filters (Pallflex Tissuequartz 2500 QAO), one Teflon membrane filter (Membrana 0.5µm pore size) and one Nuclepore filter (0.4µm pore size). Each of the quartz fiber filters was operated at an air flow rate of 10 L/min, while the Teflon filters and the Nuclepore filters were operated at 4.9 and 1.0 L/min, respectively. The quartz fiber filters were baked at 600 °C for a minimum of 2 h prior to sample collection to lower residual carbon levels associated with untreated filters.

After the sampling was completed (12 to 24 hours), the collection filter was stored in a pre-cleaned 1 L jar to which approximately 5 ml of methylene chloride was added to inhibit growth of microbes (Simoneit and Mazurek, 1982). In Gogou *et al*. (1996) and Pio *et al*. (2001), the samples were stored frozen in a pre-cleaned glass flasks sealed with teflon tape and covered with aluminium foils until further analysis.

1.4.2 Sampling pretreatment (extraction and separation)

Generally, the organic fraction of particulate matter is separated from the inorganic fraction by extraction into an organic solvent using different extraction methods (e.g.

Soxhlet extraction, ultrasonic agitation, etc.) and different organic solvents (e.g. *n*-hexane, dichloromethane, methanol, etc.).

In Pio *et al*. (2001) and Alves *et al*. (2000), the samples were extracted with dichloromethane for 24 hours. The extract was vacuum concentrated, evaporated until dryness with a nitrogen stream and weighed. The organic extracts were then subjected to fractionation by a preparative chromatographic column using silica gel and elutions with various solvents of increasing polarity.

In Sicre and Peltzer (2004), the filter papers were extracted four times in an ultrasonic bath in glass distilled methylene chloride and fractionated by silica gel chromatography. Schauer *et al*. (1996) extracted the samples twice with hexane, followed by three successive benzene-2-propanol (2:1) extractions. Extracts were combined and each final extract mixture was reduced to 200 - 500 µ1 total volume. An aliquot of the concentrated extract was derivatized with diazomethane to convert organic acids to their methyl ester analogues (Mazurek *et al.,* 1987).

Simoneit *et al*. (2000) uses Soxhlet apparatus for sample extractions. The filters were extracted with dichloromethane using Soxhlet extraction for the period of 24 hours. The extract was concentrated on a rotary evaporator system and then under a blow-down apparatus with nitrogen to about 2 ml. In Cecinato *et al*. (2000), particulate organic matter was recovered from aerosol by using a mini-soxhlet extraction device, by refluxing for 10 h with a dichloromethane-acetone mixture (DCM : Me_2CO, 5 : 1, 40 ml)

Cincinelli *et al*. (2001) adopted the method from Desideri *et al.* (1987), where they spiked the filters with internal standards (400 ng tetradecene and 200 ng di-heptylphthalate) for recovery determination. Filters were treated with a mixture of 3 ml ultrapure water and 1 ml methanol in an ultrasonic bath (Bransonic 3200, USA) for 15

min. The organic compounds were then extracted with 3 ml *n*-hexane-methylene chloride (1:1 v/v) by magnetic stirring for 15 min. The hydrophobic phase was obtained by centrifugation (5 min at 2500 rpm) and the extraction procedure was repeated three times. The second and third extracts were added to the first and the resulting solution was passed through an anhydrous sodium sulphate microcolumn and evaporated to 100 µl.

Simoneit and Mazurek (1982) treated the lipid extracts with 14% BF_3 in methanol to esterify the free acids. This step was carried out in 5 ml conical vials which contained 1.0 to 1.5 ml lipid extract plus 0.5 to 1.0 ml esterification reagent. Vials were tightly capped and then placed in an 80-85 °C water bath for 15 min. The reaction mixture was quenched with about 1 ml of doubly-distilled, chloroform-extracted water. The organic phase, containing the methylated filter extract was once again concentrated to about 100 µl and subjected to thin layer chromatography (TLC).

1.4.3 Quantification and identification

The most commonly used analytical methods for identifications of aliphatic compounds are GCMS. The fundamentals of hydrocarbons separation and analysis by GCMS are discussed below. Typical GCMS system performs six functions as follows (Peters and Moldowan, 1993):

(1) Compound separation by gas chromatography: gas-liquid chromatography accomplishes the separation by partitioning the components of a chemical mixture between an inert mobile gas phase and a non-volatile or semi-volatile stationary liquid phase held on a solid support. After the injection into the gas chromatograph, the larger molecules are retained by the stationary phase at the head of the GC column in a process called ‘cold trapping’. As the temperature of the column is gradually increased, the cold-trapped components start to move.

(2) Components are separated as they are repeatedly retained by the stationary phase and released into the mobile phase depending on their volatility and affinity.

(3) Transfer of separated compounds to the ionizing chamber of the mass spectrometer.

(4) Ionization: electron impact (EI) ionization is the most commonly used and highly developed ionization method, because it provides all the necessary spectral information required to identify an organic compound whose structure is already known. In EI ionization, each molecule eluting from the GC column is bombarded with energetic electrons having a 70eV ionizing energy (the choice of 70eV is based on the empirical observation that molecules are most efficiently ionized in the range of 50 to 90 eV) which cause it to form molecular ions (M^+).

(5) Mass analysis: the function of the mass analyzer is to separate the ions produced in the ion source according to their mass to charge ratios (*m/z*) using a magnetic or quadrapole mass spectrometer.

(6) Detection of the ions by the electron multiplier: during a scan analysis, the detector measures ions over a mass range (e.g., *m/z* 50 to *m/z* 550) at specific time (e.g., 1.5 sec). Each peak (which represents one or more compounds) eluting from the GC yields a distribution of fragment ion masses. A mass spectrum is obtained by plotting *m/z* versus response at constant scan number (related to time). A mass chromatogram (also called fragmentogram) is obtained by plotting scan number (related to GC retention time) versus response at a constant *m/z*.

(7) Acquisition, processing and display of the data by computer: GCMS analysis can be made in various operating modes including full-scans and Selected Ion Monitoring (SIM) modes. Unlike SIM, no data are lost in full-scan GCMS, but

extensive computer storage is required. Hence, all mass spectra needed for compounds identification can be generated from full-scan analysis.

1.5 OBJECTIVES

The main objectives of this study are: (a) to determine the composition of extracted lipids from airborne particulate samples of Straits of Malacca, South China Sea and Sulu-Sulawesi Seas, (b) to determine the sources of organic matter in the particulate samples, and (c) to determine the sources of organic matter in the particulate samples based on molecular marker.

2

EXPERIMENTAL

2.1 SAMPLING SITES

26 samples were taken from sites near the coastal area of Straits of Malacca, South China Sea and Sulu-Sulawesi Seas. Figure 2.1 and Table 2.1 show the sampling sites and its coordinates.

Scale: 1 cm:10km

Figure 2.1: Map of the sampling sites.

From Figure 2.1, we can see the location of the sampling sites. Sampling site 1-7 are near Sarawak, sampling site 8 and 9 are in the Straits of Malacca, where sampling site 8 is near Malacca and sampling site 9 is near to Batam Island, where the industrial areas are. Sampling site 10 is near the Labuan Island. This is also an industrial area. Sampling site 11-13 is deeper to the South China Sea. Sampling site 14 and 15 are near to the coastline of Sabah. Sampling site 16 to 26 is in the Sulu-Sulawesi Seas. Most of the sampling was done in the late evening, and taken for 24 hours.

Table 2.1: Coordinates, date and time taken for all sampling sites.

Sample	Coordinate	Date & time taken	Sample	Coordinate	Date & time taken
1	N 02° 28.333' E 109° 20.068'	20/06/09, 6.05PM	14	N 06° 09.044' E 116° 02.700'	14/07/09, 6.40PM
2	N 03° 19.644' E 110° 31.069'	21/06/09, 6.10PM	15	N 07° 10.628' E 116° 59.022'	15/07/09, 6.00PM
3	N 03° 53.216' E 110° 52.797'	22/06/09, 6.51PM	16	N 06° 42.759' E 117° 49.790'	16/07/09, 6.15PM
4	N 04° 20.544' E 111° 32.583'	23/06/09, 6.34PM	17	N 06° 23.596' E 117° 55.488'	17/07/09, 5.40PM
5	N 03° 56.476' E 112° 28.851'	25/06/09, 7.00PM	18	N 06° 17.148' E 118° 10.540'	18/07/09, 11.30PM
6	N 05° 25.437' E 112° 14.220'	26/06/09, 6.45PM	19	N 05° 46.327' E 118° 42.308'	19/07/09, 6.33PM
7	N 06° 19.024' E 112° 24.509'	27/06/09, 6.15PM	20	N 05° 42.858' E 119° 08.598'	20/07/09, 7.27PM
8	N 02° 24.686' E 101° 36.402'	18/06/09, 5.14PM	21	N 04° 13.349' E 118° 38.937'	26/07/09, 11.45AM
9	N 01° 43.664' E 105° 09.222'	19/06/09, 6.45PM	22	N 07° 03.682' E 117° 28.069'	30/07/09, 7.00PM
10	N 05° 29.606' E 115° 17.668'	01/07/09, 5.30PM	23	N 04° 10.745' E 118° 26.936'	22/07/09, 12.05PM
11	N 07° 21.657' E 113° 50.452'	04/07/09, 6.50PM	24	N 04° 53.940' E 118° 36.221'	27/07/09, 6.45PM
12	N 07° 54.310' E 114° 04.730'	06/07/09, 7.00PM	25	N 05° 33.257' E 119° 02.373'	28/07/09, 6.00PM
13	N 07° 56.651' E 113° 54.615'	07/07/09, 6.00PM	26	N 04° 09.776' E 117° 58.583'	21/07/09, 7.07PM

2.1.1 Straits of Malacca

The Straits of Malacca is a narrow, 805 km stretch of water between Peninsular Malaysia and the Indonesian island of Sumatera. It is named after the Empire of Melaka that ruled over the archipelago in the period of 1414 to 1511. Straits of Malacca, linking the Indian Ocean with the South China Sea, are one of the world's most important sea passages. Chief ports include Belawan in Indonesia, Melaka and Penang in Malaysia, and Singapore at the southern end of the strait.

In the south of the strait, water depths rarely exceed 120 feet (37 metres) and are usually about 90 feet (27 metres). Toward the northwest, the bottom gradually deepens until it reaches to about 650 feet (200 metres) as the strait merges with the Andaman Basin. Numerous islets, some fringed by reefs and sand ridges, hinder passage at the southern entrance to the strait. The sand ridges are identified as accumulations of material that have been brought down by rivers from Sumatra.

This Straits supplies myriads of marine resources and supports the economy of the littoral states. More than 380,000 tonnes of fish (more than 60% of the total fish caught per year) costing RM1.2 billion per year is landed from the Straits of Malacca. In Indonesia, The Straits of Malacca contributes the second highest fish production after the Java Sea (MASDEC website). High quality and safe fish harvest is extremely important to ensure sustainable socio-economic development and health of the people. Other economic activities such as mariculture, tourism, recreation and maritime industry are dependent on the viability and pristine conditions of the Straits. The Straits is also an important site for archaeological resources (TED Case Study).

Coastal swamps are commonly found on both sides of the strait, and a huge, low-lying swamp forest lies along the eastern coast of Sumatra. The strait is silting on both sides, and, near the mouths of large rivers, silt accretions range from about 30 feet

(9 metres) on the coast of Malaya to about 650 feet annually on the east coast of Sumatra.

The climate of the strait is hot and humid and is characterized by the northeast monsoon during the (northern) winter and the southwest monsoon during the summer. The average annual rainfall varies between 76 inches (1,930 mm) and 101 inches (2,570 mm). Throughout the year, the current flows northwest through the strait. Surface-water temperatures in the strait are 87 to 88 °F (30.6 to 31.1 °C) in the east and may be as much as 4 °F (2.2 °C) lower in the west. The close proximity of land and the discharge of large rivers result in a low salinity for the strait (Britannica Online Encyclopedia).

2.1.2 South China Sea

The South China Sea is part of the Pacific Ocean, stretching roughly from Singapore and the Straits of Malacca in the southwest, to the Strait of Taiwan (between Taiwan and China) in the northeast. The area includes more than 200 small islands, rocks, and reefs, with the majority located in the Paracel and Spratly Island chains. There are many islands, beautiful coral reefs, and all kinds of marine animals in the South China Sea, giving it the perfect conditions to develop the tourist industry (South China Sea Virtual Library).

The South China Sea is an extremely significant body of water in a geopolitical sense. It is the second most used sea lane in the world, while in terms of world annual merchant fleet tonnage, over 50% passes through the Straits of Malacca, the Sunda Strait, and the Lombok Strait. The region has proven oil reserves of around 1.2 km^3 (7.7 billion barrels), with an estimation of 4.5 km^3 (28 billion barrels) in total. Natural gas reserves are estimated to total around 7,500 km^3 (266 trillion cubic feet) (Tønnesson, 2005).

According to the studies made by the Department of Environment and Natural Resources, Philippines, this body of water holds one third of the all world's marine biodiversity, making it a very important area for the ecosystem. It has a wide variety of sea life, including coral, tropical fish, sea anemones etc. There are also natural gas, petroleum and all kinds of marine products (Discovering South China Sea).

2.1.3 Sulu-Sulawesi Sea

The Sulu-Sulawesi Sea is oceanographically well defined, by the Palawan through to the north and by a promontory from Sulawesi Island to the south, and the Bohol Sea between the Visayas and northern Mindanao (DeVantier *et al*., 2004).

The Sea, with its terrestrial, coastal and marine ecosystems, lies within the global center of tropical biodiversity (Chou, 1997). The sea has more than 500 species of reef-building corals and 2500 species of marine fishes. Five species of sea turtles (Green, Hawksbill, Olive Ridley, Loggerhead and Leatherback) and at least 22 species of marine mammals occur, including Sperm Whales and Dugongs, present in Palawan and Sarangani provinces, Philippines (DeVantier *et al*., 2004).

Many of the coastlines of Sulu-Sulawesi Seas were originally fringed by mangrove forests, seagrass beds, and coral reefs. Fringing reefs are very well developed, away from the major river estuaries. Nowadays, the ecoregion of the sea suffer from dynamite fishing, overfishing, coastal development, sedimentation, and coral bleaching. Human population density, amongst the highest in the world, leads to a severe impact on marine ecosystems from overexploitation, pollution and coastal development.

2.2 REAGENT, GLASSWARE AND APPARATUS

All solvent used were of HPLC grade. Dichloromethane, *n*-hexane and methanol were obtained from Merck (Germany). Water for deactivation of silica and alumina was

prepared by deionizing distilled water (Maxima Ultra-pure water, Elgastat Maxima, ELGA, England). Alumina (70-230 mesh) and silica gel (40-60 μm, PhamPrep 60 CC) were obtained from Merck (Germany).

All glassware used in analytical work was soaked in 3% (v/v) Extran MA03 (Merck, Germany) overnight, rinsed with distilled water, dried in the oven at 200°C overnight, wrapped with aluminum foil, and rinsed with methanol and dichloromethane before use.

Alumina and silica gel were cleaned as follows: (a) 30 minutes sonication with methanol, (b) drying the residual of methanol, (c) 30 minutes sonication with *n*-hexane and (d) further cleaning with dichloromethane-methanol (9:1) using three times 15 minutes sonication. Glass wool and anhydrous sodium sulphate were cleaned three times by sonication for 15 minutes period each with methanol and cleaning repeated with dichloromethane.

Ultrasonic bath (WiseClean, Wisd Laboratory Instrument) was used for sample extraction and rotary evaporator system (Büchi, Switzerland) was used for the concentration steps.

2.3 PREPARATION OF STANDARDS

2.3.1 Internal standards

Tetracosane-d_{50} (98% purity) was obtained from Isotec (USA). Tetracosane-d_{50} stock solution (121.52 μg/ml) was prepared by accurately weighing 6.20 mg of solid tetracosane-d_{50}, dissolved in *n*-hexane and quantitatively transferred to a 50 ml volumetric flask and made up to the mark with *n*-hexane.

2.3.2 External standards

All external standards were obtained from Sigma-Aldrich, Switzerland.

2.3.2.1 *n*-Alkanes

Two mixtures of C_{10}-C_{20} and C_{21}-C_{40} *n*-alkanes standards were used (Table 2.2) throughout the analytical work.

Table 2.2 : The *n*-alkanes standard used in this research.

No.	Compound	Concentration (µg/ml)	Compound	Concentration (µg/ml)
1	Decane ($C_{10}H_{22}$)	100	Hexacosane ($C_{26}H_{54}$)	100
2	Undecane ($C_{11}H_{24}$)	100	Heptacosane ($C_{27}H_{56}$)	100
3	Dodecane ($C_{12}H_{26}$)	100	Octacosane ($C_{28}H_{58}$)	100
4	Tridecane ($C_{13}H_{28}$)	100	Nonacosane ($C_{29}H_{60}$)	100
5	Tetradecane ($C_{14}H_{30}$)	100	Tricontane ($C_{30}H_{62}$)	100
6	Pentadecane ($C_{15}H_{32}$)	100	Hentriacontane ($C_{31}H_{64}$)	100
7	Hexadecane ($C_{16}H_{34}$)	100	Dotriacontane ($C_{32}H_{66}$)	100
8	Heptadecane ($C_{17}H_{36}$)	100	Tritracontane ($C_{33}H_{68}$)	100
9	Octadecane ($C_{18}H_{38}$)	100	Tetratriacontane ($C_{34}H_{70}$)	100
10	Nonadecane ($C_{19}H_{40}$)	100	Pentatriacontane ($C_{35}H_{72}$)	100
11	Eicosane ($C_{20}H_{42}$)	100	Hexatriacontane ($C_{36}H_{74}$)	100
12	Heneicosane ($C_{21}H_{44}$)	100	Heptatriacontane ($C_{37}H_{76}$)	100
13	Docosane ($C_{22}H_{46}$)	100	Octatriacontane ($C_{38}H_{78}$)	100
14	Tricosane ($C_{23}H_{48}$)	100	Nonatriacontane ($C_{39}H_{80}$)	100
15	Tetracosane ($C_{24}H_{50}$)	100	Tetracontane ($C_{40}H_{82}$)	100
16	Pentacosane ($C_{25}H_{52}$)	100		

2.3.2.2 *n*-Aldehyes

Because of the lack of standards, four *n*-aldehydes (Table 2.3) were used as standards throughout the analytical work.

Table 2.3: The *n*-aldehydes standard used in this research.

No.	Compound	Concentration (µg/ml)	Compound	Concentration (µg/ml)
1	Hexadecanal ($C_{16}H_{32}O$)	100	Eicosanal ($C_{20}H_{40}O$)	100
2	Octadecanal ($C_{18}H_{36}O$)	100	Tetracosanal ($C_{24}H_{48}O$)	100

2.3.2.3 *n*-Alkan-2-ones

Tetradecan-2-one, nonadecan-2-one and hentriacontan-2-one were used as *n*-alkan-2-ones standards (Table 2.4) throughout the analytical work.

Table 2.4: The *n*-alkan-2-ones standard used in this research.

No.	Compound	Concentration (µg/ml)	Compound	Concentration (µg/ml)
1	Tetradecan-2-one ($C_{14}H_{28}O$)	100	Hentriacontan-2-one ($C_{31}H_{62}O$)	100
2	Nonadecan-2-one ($C_{19}H_{38}O$)	100		

2.3.2.4 *n*-Alkan-1-ols

Five long chain *n*-alkan-1-ols were used as standards (Table 2.5) for the analytical work.

Table 2.5: The *n*-alkan-1ols standard used in this research.

No.	Compound	Concentration (µg/ml)	Compound	Concentration (µg/ml)
1	Hexadecan-1-ol ($C_{16}H_{34}O$)	100	Tetracosan-1-ol ($C_{24}H_{50}O$)	100
2	Octadecan-1-ol ($C_{18}H_{38}O$)	100	Heptacosan-1-ol ($C_{27}H_{56}O$)	100
3	Eicosan-1-ol ($C_{20}H_{42}O$)	100		

2.3.2.5 *n*-Alkan-1-oic acids

Because of the lack of standards for long chain *n*-alkan-1-oic acids, six fatty acids compounds (Table 2.6) were obtained and were used throughout the analytical work.

Table 2.6: The *n*-alkan-1-oic acids standard used in this research.

No.	Compound	Concentration (μg/ml)	Compound	Concentration (μg/ml)
1	Nonanoic acid ($C_9H_{18}O_2$)	100	Eicosanoic acid ($C_{20}H_{40}O_2$)	100
2	Dodecanoic acid ($C_{12}H_{24}O_2$)	100	Tetracosanoic acid ($C_{24}H_{48}O_2$)	100
3	Hexadecanoic acid ($C_{16}H_{32}O_2$)	100	Heptacosanoic acid ($C_{27}H_{54}O_2$)	100

2.4 SAMPLING AND SAMPLE PREPARATION

Airborne particulate samples were acquired with standard high volume air sampler and 10 micron selective inlet (Ecotech 2000, Australia) fitted with glass fiber filters (20.3 cm x 25.4 cm surface, Whatman EPM 2000, England) operated at a flow rate of 1.13 m^3/min for a sampling period of 24 hours.

Prior to sampling, the glass fiber filters were wrapped with aluminum foil, equilibrated in a desiccator (<30% relative humidity) for at least 24 hours, and weighted.

2.5 EXTRACTION

Extraction of the air particulate samples was performed with dichloromethane using 15 minutes sonication for three times. The extracts were then filtered through sintered glass funnel for the removal of insoluble particles. The filtrate was concentrated to approximately 1 ml by using a rotary-evaporator system, transferred to a pre-weighed vial and then evaporated to dryness. The volume was readjusted to 1 ml exactly by addition of dichloromethane, evaporated to dryness using a stream of dry nitrogen gas, and quantified by weighing the dry aliquot on an analytical balance.

2.6 FRACTIONATION

Fractionation was carried out using self packed alumina-silica column. Alumina and silica gel were first activated at 200°C for 4 hours and then partially deactivated 5% (w/w) using deionized water. The glass column (1.0 cm I.D) was slurry packed with 5 g silica gel (bottom) using *n*-hexane and dry packed with 10 g alumina (top) supported by a small plug of pre-cleaned glass wool inserted at the narrow end of the column. The absorbents were capped with 1.0 g of anhydrous sodium sulphate to form a protective surface layer. 1 ml of the extract was applied to the top of the column.

Elution was performed using 20 ml of *n*-hexane to yield the first fraction (F1) containing the aliphatic hydrocarbons. Then with 30 ml of 10% dichloromethane in *n*-hexane and 20 ml of 50% dichloromethane in *n*-hexane to yield second fraction (F2). For the third fraction (F3), elution was performed with 40 ml of 10% methanol in dichloromethane. The first and second fractions (F1 and F2) were concentrated to approximately 100 µl under reduced pressure at 40°C using a rotary-evaporator system. The volume was then adjusted to 100 µl exactly by addition of *n*-hexane (first fraction) and dichloromethane (second fraction). For the third fraction, aliquots were converted to trimethylsilyl derivatives by reaction with BSTFA (N, O-bis(trimethylsilyl)trifluoroacetamide) and TCMS (trimethylchlorosilane) for 4 hours at 70 °C before GCMS analysis.

2.7 INSTRUMENTAL ANALYSIS

Instrumental analysis was performed using Shimadzu GCMS-QP2010 Plus gas chromatography mass spectrometer with splitless injector and Rtx. 5MS column (30 m long, 0.25 mm I.D and 0.25 µm film thickness). Helium (99.999% purity) was used as carrier gas. The chromatographic conditions are given in Table 2.7. The data for

quantitative analysis was acquired from electron impact (EI) mode (70 eV) scanning from 50 to 700 a.m.u at 1.4 sec/scan.

Table 2.7: Chromatographic condition of GCMS.

Oven temperature program	Initial oven temperature 70 °C, hold for 2 minutes; then up to 150 °C at 30 °C/min, increase to 310 °C at 4 °C/min, then held at 310 °C for 10 mins.
Gas flow rate	1.20 ml/min
Injection port temperature	300 °C
Injection mode	Splitless
Column inlet pressure	77.0 kPa
Average velocity	40.2 cm/s
Temperature of transfer line	310 °C
Solvent delay	4 mins

All quantifications were based on the compound area derived from the ion fragmentogram shown in Table 2.8.

Table 2.8: Key fragment ions for mass spectrometric characterization of hydrocarbons.

No.	Compound	Key fragment ion (*m/z*)
1	*n*-Alkanes	85
2	*n*-Aldehydes	82, 96
3	*n*-Alkan-2-ones	59, 71
4	*n*-Alkan-1-ols	73, 103
5	*n*-Alkan-1-oic acids	117

The outlines of the calculations to determine the compounds concentration in the studied samples are shown below.

$$Conc = \frac{Amt}{V}$$

where,

$$Amt = [(RF_{avg} \times Area \times V_{binj}) / (V_{inj} \times V_{extc}) / (V_{frc} - A_{contm})] / (R/100)$$

where,

Amt is the amount of compound corrected to blank and recovery.

RF_{avg} is the average response factor ($RF_{avg} = Conc_{ext} \times V_{inj} / Area_{ext}$)

where,

$Conc_{ext}$ is the concentration of the external standards,

V_{inj} is the injection volume,

$Area_{ext}$ is the area of the external standard in the fragmentogram.

All areas refer to the peak area of the compound in the fragmentogram.

V_{binj} is the total volume of the extract,

V_{extc} is the volume of the extract,

V_{frac} is the volume of the extract used for fractionation,

A_{contm} is the amount of contamination ($A_{contm} = Conc_{contm} \times V_{extr}$)

where,

$Conc_{contm}$ is the contamination concentration

V_{extr} is the total volume of extract of the sample to be corrected,

R is the recovery,

V is the volume of air sampled (m^3).

2.8 PROCEDURAL BLANKS

Procedural blanks for the air particulate samples were analyzed and quantified. Procedural blanks analysis was carried out by extracting a blank filter paper with dichloromethane in a clean conical flask followed by fractionation and GCMS analysis. The experiment was repeated three times.

Solvent blanks (450 ml of dichloromethane and 50 ml of *n*-hexane concentrated to 100 μl) were also analyzed in order to monitor the backgrounds. The amounts of contaminants that have been quantified were subtracted from those real samples in order to assess the actual concentration of the compound.

3

RESULTS AND DISCUSSION

3.1 GENERAL CHARACTERISTIC OF OCEANIC AIR PARTICLES

3.1.1 Total extracted lipids in air particulate matter

The concentration of extracted lipids in air particulate samples is presented in Table 3.1.

Table 3.1: Concentrations of extracted lipids in the air particulate samples.

Sample	Conc. of total extract ($\mu g/m^3$)
1	1.523
2	0.574
3	1.393
4	0.819
5	1.188
6	0.410
7	1.004
8	0.963
9	1.270
10	0.778
11	1.045
12	0.553
13	0.307
14	0.676
15	0.656
16	0.737
17	0.287
18	0.492
19	0.225
20	0.594
21	0.615
22	1.311
23	0.778
24	0.819
25	0.574
26	3.134

Lipids are fractions of organic matter which can be isolated by extraction with organic solvents. Extraction of air particulate matter in this study yields hydrocarbons and the hydrocarbon-like fatty acids, alcohols, ketones and aldehydes. The extracted lipid concentrations for air particulate samples vary from 0.225 μg/m^3 to 3.134 μg/m^3.

3.2 DIAGNOSTIC PARAMETERS AND CALCULATIONS

3.2.1 Carbon Preference Index (CPI)

The Carbon Preference Index (CPI), a measure of the carbon number predominance, is useful to determine the degree of biogenic versus petrogenic input (Mazurek and Simoneit, 1984).

Carbon Preference Index (CPI_1) for whole range of *n*-alkanes was calculated as follows:

$$CPI_1 = \frac{\sum C_{13} - C_{35}}{\sum C_{12} - C_{34}} \quad \text{.....Equation 3.1}$$

For higher plant wax *n*-alkanes, CPI_2 was calculated as follows (Zhu *et al*., 2005):

$$CPI_2 = \frac{\sum C_{25} - C_{33}}{\sum C_{26} - C_{34}} \quad \text{.....Equation 3.2}$$

Split range for bacterial, algal *n*-alkanes (Simoneit, 1989):

$$CPI = \frac{\sum C_{11} - C_{25}}{\sum C_{10} - C_{24}} \quad \text{.....Equation 3.3}$$

Carbon Preference Index for *n*-aldehydes was calculated as follows:

$$CPI = \frac{1}{2}\left[\frac{\sum C_{even} + C_{even}}{\sum C_{odd}}\right] \quad \text{.....Equation 3.4}$$

Carbon Preference Index for *n*-alkan-2-ones was calculated as follows:

$$CPI = \frac{2\sum C_{odd}}{\sum C_{even} + \sum C_{even}} \quad \text{.....Equation 3.5}$$

Carbon Preference Index for *n*-alkan-1-ols and *n*-alkan-1-oic acids was calculated as follows (Gogou *et al*., 1996):

$$CPI = \frac{C_{even}}{C_{odd}} \quad \text{.....Equation 3.6}$$

3.2.2 Carbon Number Maximum (C_{max})

The carbon number maximum of the most abundant *n*-alkanes (C_{max}) can also be used as an indicator of relative source input (Mazurek and Simoneit, 1984). Carbon number maximum was chosen from the distribution diagrams of *n*-alkanes.

Hostettler *et al*. (1989) proposed the use of C_{max} values for *n*-alkanes (C_{29}) and *n*-aldehydes (C_{30}) as a fact to propose the possible precursor product relation between these compounds. They concluded that the *n*-alkanes were derived from decarbonilation of *n*-aldehydes.

3.2.3 Average Chain Length (ACL)

ACL of *n*-alkanes (C_{23}-C_{33}) can be useful in showing changing sources of organic carbon and has also been used as an indicator of paleoclimatic information in marine settings (Poynter *et al*., 1989).

ACL for C_{23} to C_{33} were calculated based on *n*-alkanes concentration as follows (Theissen *et al.*, 2005):

$$ACL = \frac{(i \times \sum[C_i])}{\sum[C_i]} \quad \text{.....Equation 3.7}$$

Where *i* is either 23, 24 to 32 or 33 and $[C_i]$ is the concentration of *n*-alkanes.

ACL also can be used to identify *n*-alkyl lipids from different vegetation (Ternois *et al*., 2001; Boot *et al*., 2006; Jeng, 2006). Vegetation types are the main influence on chain length of terrigenous leaf lipids. For example, leaf lipids derived from grasslands may have longer chain lengths on average than leaf lipids from plants in forests (Cranwell, 1973).

3.2.4 Plant wax *n*-alkanes

The 'signature' of natural wax *n*-alkanes (from higher plants), was introduced by Simoneit *et al.,* (1990a). The plant wax *n*-alkanes can be estimated from the following equation (Simoneit *et al*., 1991a):

Wax $C_n = C_n - 0.5\,[C_{n+1} + C_{n-1}]$ …….Equation 3.8

where n = 25, 27, 29, 31, 33.

Negative values were taken as zero.

3.2.5 Higher Plant Alkane Index (HPA)

The higher plant alkane index (HPA) has been used as a degradation signal to estimate the extent of degradation of *n*-alkanols (Poynter and Eglinton, 1991; Jeng and Huh, 2001). HPA is defined as:

$$\mathrm{HPA} = \frac{\sum C_{24}, C_{26}, C_{28}\ n\text{-alkan-1-ols}}{\left(\sum C_{24}, C_{26}, C_{28}\ n\text{-alkan-1-ols}\right) + \left(\sum C_{27}, C_{29}, C_{31}\ n\text{-alkanes}\right)}$$ …….Equation 3.9

The main assumption of using HPA index is that the ratio of primary fluxes of long chain *n*-alkanes and *n*-alkanols is approximately constant over the total study area.

3.2.6 Alcohol Index (AI)

Alcohol index (AI) was used to evaluate the relationship between *n*-alkanols and *n*-alkanes (Cacho *et al*., 2000). AI is defined as

$$\mathrm{AI} = \frac{n - \text{hexacosan-1-ol}}{n - \text{nonacosane} + n\text{-hexacosan-1-ol}}$$ …….Equation 3.10

3.2.7 Lower Molecular Weight to Higher Molecular Weight ratio (LMW/HMW ratio)

LMW/HMW ratio can be used to determine the contribution of marine and terrigenous inputs to the environmental sample. LMW/HMW can be calculated from the following equation (Gao *et al*., 2008):

$$\text{LMW/HMW} = \frac{\sum n-C_{15\text{-}21}}{\sum n-C_{22\text{-}36}} \quad \text{.....Equation 3.11}$$

3.3. *n*-ALKANES

3.3.1 *n*-Alkanes sources

Crude petroleum, the primary source of gasoline, diesel fuel and lubricating oil contains *n*-alkanes ranging up to about C_{35} with essentially no carbon number predominance (CPI ~ 1) (Simoneit, 1984). Gasoline fuel is composed of hydrocarbons mainly ranging from C_5 to C_{10}. In diesel fuel, 95% of *n*-alkanes are < C_{19} (Hauser and Pattison, 1972). Lubricating oil derived from petroleum contains minor amount of *n*-alkanes (Simoneit, 1985).

During engine operation, the temperature is raised to ~ 250 °C. This will cause *n*-alkyl hydrocarbons to undergo mild thermocracking, usually at the tertiary carbon atoms. This may explain the presence of high molecular weight *n*-alkanes in vehicular exhaust even when the fuel and the lubricating oils were originally deficient in those compounds. (Rogge *et al*., 1993).

Plant wax *n*-alkanes ranges from about C_{21} to C_{37} (Tulloch, 1976). *n*-Alkanes are biosynthesized by head-to-head condensation of two fatty acids, followed by decarboxylation to the ketone, reduction to secondary alcohol, then dehydration and reduction to give *n*-alkanes (Kolattukudy *et al*., 1976).

n-Alkanes with an even number of carbon atoms can only result from the coupling of fatty acids containing an even number and odd number carbon atoms. Because odd carbon number fatty acids are relatively rare, virtually odd carbon number *n*-alkanes are predominant in plants (Bird and Lynch, 1974).

3.3.2 *n*-Alkanes characterizations

n-Alkanes were characterized on *m/z* 85 fragmentogram (Figure 3.1). *n*-Alkanes in air particulate samples are in the range of C_{14}-C_{36}. Their concentrations vary from 0.03 ng/m^3 to 6.06 ng/m^3. *n*-Alkanes is not detected in Sample 19 (Table 3.2). The highest *n*-alkanes concentration observed is in Sample 1, while the lowest is in Sample 11. These *n*-alkanes values are close to those measured in aerosol samples collected form Ninety Mile Beach, New Zealand (Sicre and Peltzer, 2004). High concentration of *n*-alkanes in Sample 1, coupled with low CPI value is most probably due to contamination from the vehicular emission of the ship engine.

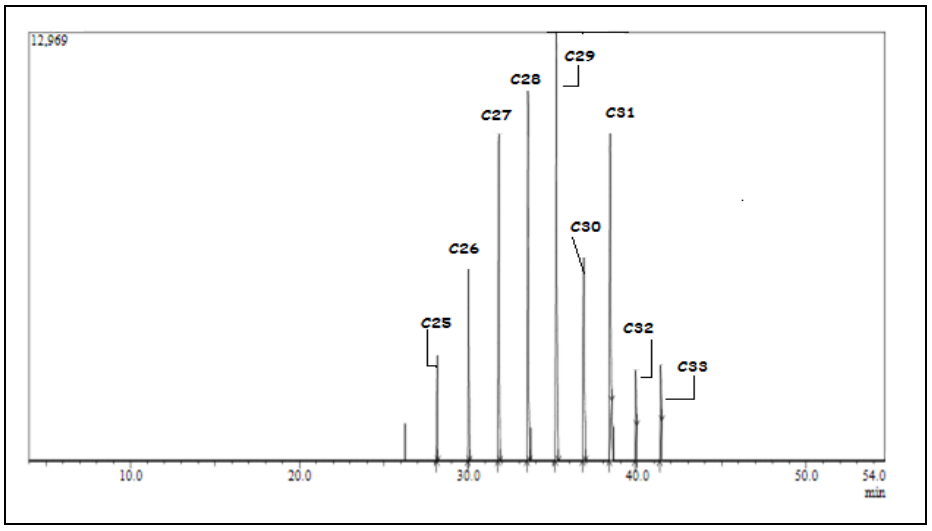

Figure 3.1: *m/z* 85 fragmentogram for the air particulate sample (S1).

Table 3.2: Total *n*-alkanes concentration for air particulate samples.

Sample	Conc. of *n*-alkanes (ng/m^3)
1	6.06
2	0.61
3	3.04
4	0.10
5	0.11
6	0.07
7	0.15
8	1.21
9	1.83
10	0.12
11	0.06
12	0.11
13	0.11
14	0.10
15	0.13
16	0.21
17	0.13
18	0.09
19	n.d
20	0.05
21	0.34
22	0.17
23	0.11
24	0.18
25	0.04
26	0.03

*n.d = not detected

The carbon preference index (CPI) of *n*-alkanes is often used to estimate relative contributions from higher plant waxes and fossil fuel hydrocarbons to these homologues. This is because the CPI values of higher plant wax *n*-alkanes are generally >5 when there is no serious input from pollutant, but the values tend to decrease down to 1.0 with an increase of contribution from anthropogenic sources (Yamamoto *et al*., 2011). CPI_1 represents odd-over even carbon number for the whole range of identified

and quantified *n*-alkanes while CPI_2 represents *n*-alkanes in the range of higher plant wax *n*-alkanes. The purpose of plotting and calculating these two parameters is to study the contribution of higher plant wax *n*-alkanes to the whole range of *n*-alkanes. The CPI_1 values for most of the samples are low (<2.5) (Table 3.3). Low CPI values observed reflects clearly the significant contribution of even carbon chain length *n*-alkanes to odd carbon chain, which indicate a major contribution from petroleum residues. Almost half of the air particulate samples have the relatively high (>1.9) CPI_2 value. CPI for bacterial and algal in almost all the samples are quite high (>2). These data indicate important input from marine bacteria and algae.

Table 3.3: CPIs value for *n*-alkanes in air particulate samples.

Sample	CPI_1	CPI_2	CPI for bacterial, algal
1	1.4	1.4	4.0
2	4.5	2.7	n.a
3	1.8	1.4	8.6
4	2.2	2.5	2.9
5	2.1	1.3	6.8
6	0.7	4.0	0.7
7	2.2	2.6	4.1
8	1.5	1.5	2.1
9	1.4	1.4	12.5
10	1.9	2.8	2.5
11	1.3	1.6	1.8
12	1.0	1.1	1.3
13	1.0	1.4	1.2
14	2.2	3.2	2.2
15	2.5	3.1	2.2
16	1.2	1.5	1.4
17	1.9	2.1	1.8
18	2.1	2.4	2.7
19	n.a	n.a	n.a
20	2.1	2.3	2.5
21	1.6	1.8	1.5
22	1.2	1.2	3.9
23	1.5	1.7	0.8
24	2.0	3.0	1.6
25	1.4	1.6	1.6
26	1.6	2.7	1.5

*n.a = not available

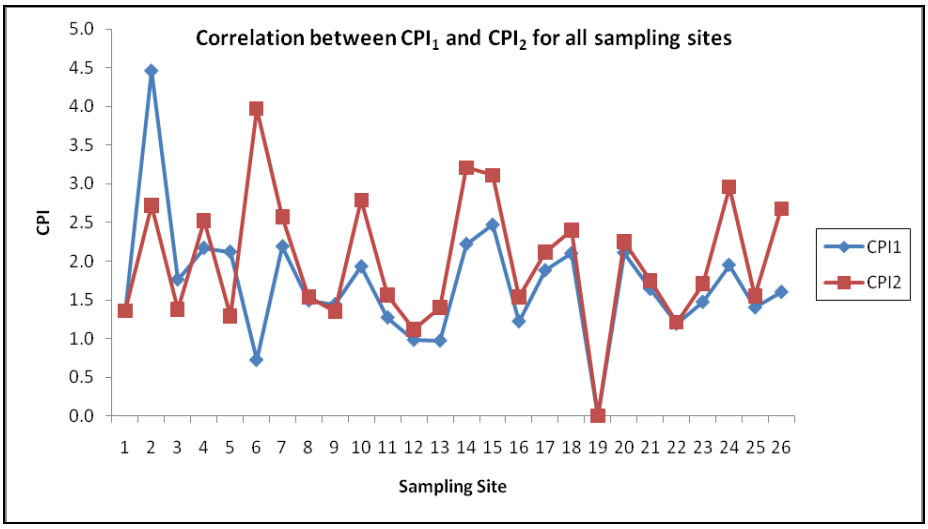

Figure 3.2: Correlation between CPI_1 and CPI_2 for all sampling sites.

The distribution pattern of *n*-alkanes at all sampling sites (Figure 3.3) were almost similar, maximizing at C_{21}, C_{27} and C_{31}. These long chain *n*-alkanes (C_{27} and C_{31}) have been attributed to terrestrial higher plants. Small amounts of short chain *n*-alkanes (C_{17} to C_{20}) were also present in the air particulate samples. This short chain chain *n*-alkanes have been suggested to be derived from algae. Saliot (1981) and Parish (1988) reported that the major *n*-alkanes in bacteria and phytoplankton are dominated by odd-numbered carbons ranging from C_{15} to C_{21}. Ishiwatari *et al*. (2005) also suggested that the *n*-alkanes ranging from C_{17} to C_{20} as plankton-derived *n*-alkanes.

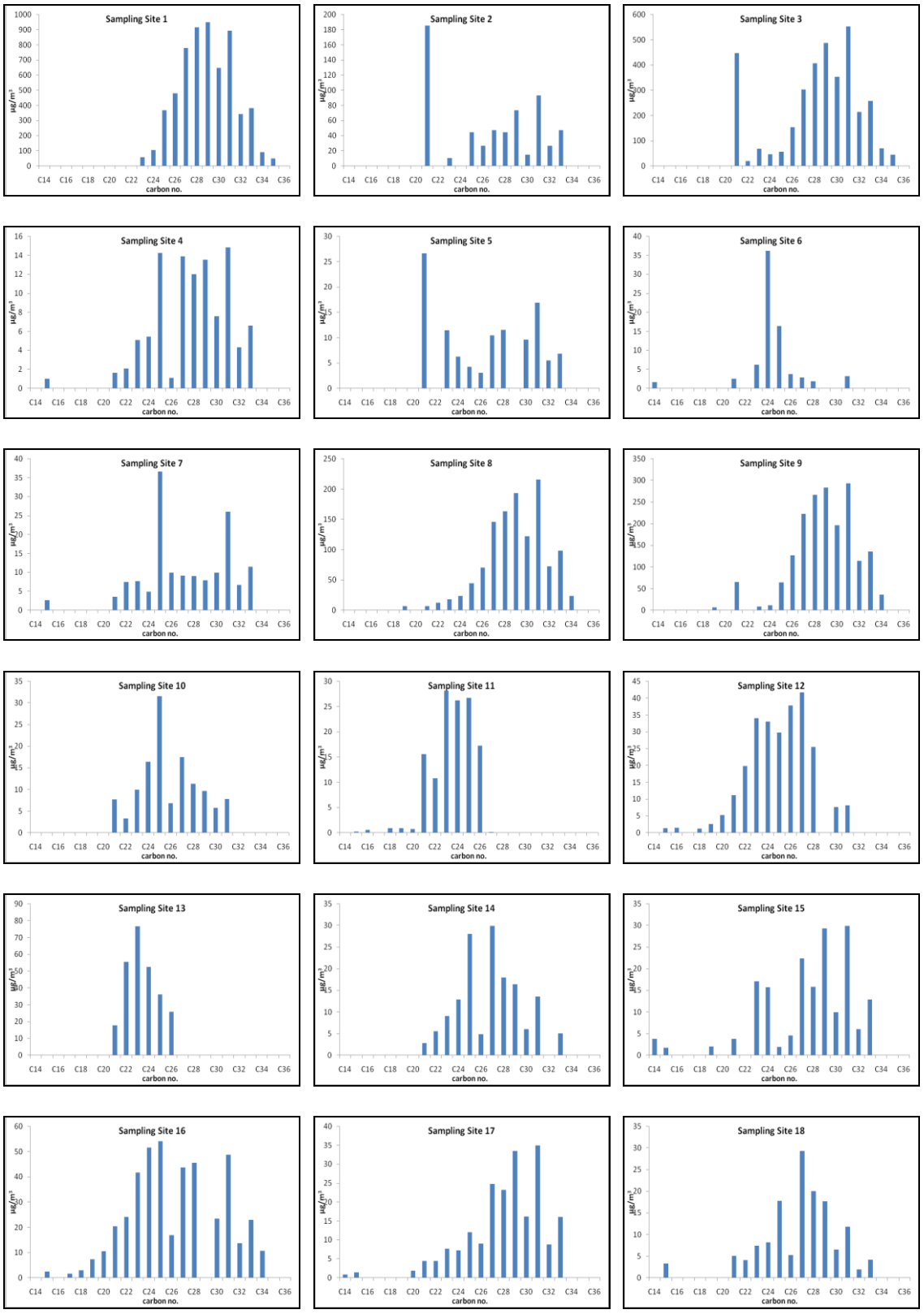

Figure 3.3: Distribution of *n*-alkanes concentration in air particulate sample (Distribution for sampling site 19 is not available)

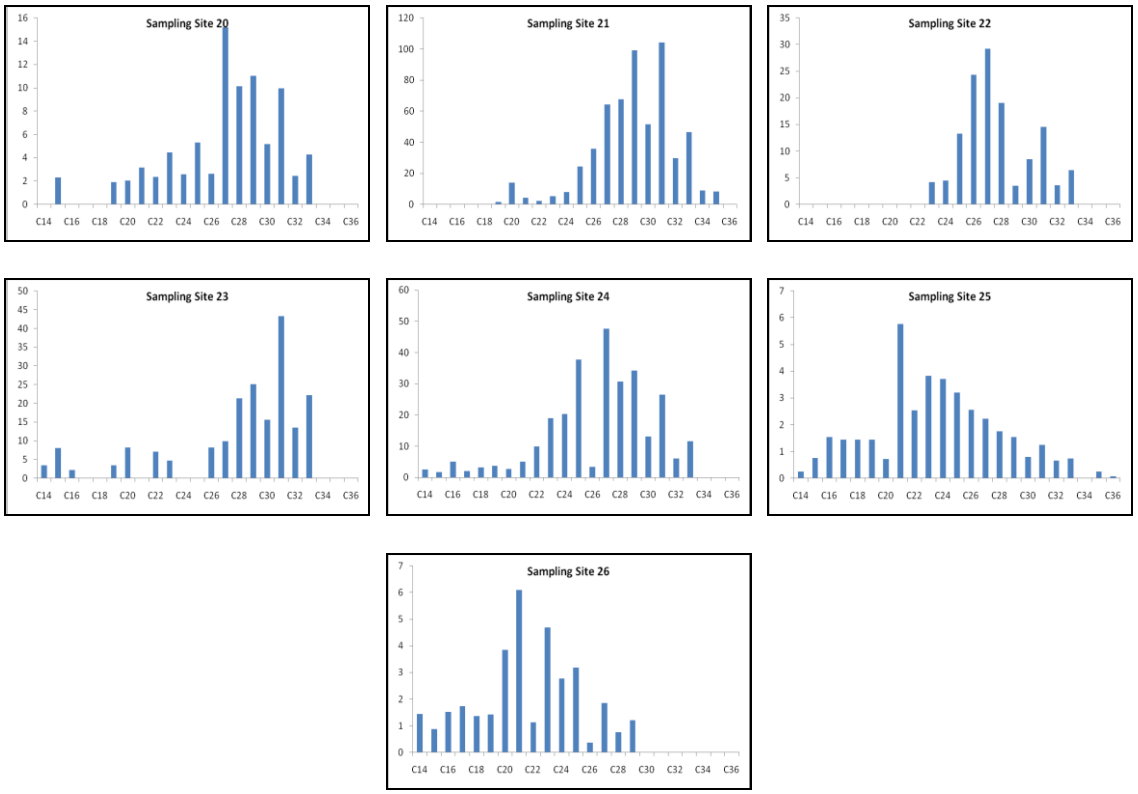

Figure 3.3 (cont.): Distribution of *n*-alkanes concentration in air particulate sample (Distribution for sampling site 19 is not available)

The Average chain length (ACL) of *n*-alkanes can be useful in showing changing sources of organic matter in environmental samples. Table 3.4 shows the ACL value for all air particulate samples. The ACL value for most of the samples is high, ranging from 24.1 to 29.8. High ACL value (≥ 27) indicates a greater contribution of terrestrial plant wax. Based on the sampling map (Figure 2.1, page 11), most sampling sites with high ACL value are located near the coastal area, where many species of plant exist. ACL value below than that simply shows that the sources of *n*-alkanes in air particulate samples comes from other sources like petroleum combustion and marine plankton or algal.

Table 3.4: ACL values of *n*-alkanes for air particulate samples.

Sample	ACL for *n*-alkanes
1	28.9
2	29.0
3	29.4
4	28.2
5	28.2
6	24.8
7	28.0
8	29.2
9	29.2
10	26.3
11	24.3
12	25.8
13	24.1
14	27.1
15	28.0
16	27.4
17	28.7
18	27.5
19	n.a
20	28.2
21	29.2
22	27.7
23	29.8
24	27.5
25	26.3
26	24.9

*n.a = not available

The contribution of plant wax *n*-alkanes was calculated using equation 3.8 (Page 26, section 3.2.4). Based on the equation, plant wax concentration of *n*-alkanes with carbon number 23, 25, 27, 29, 31 and 33 was calculated and hence the contribution of biogenic source estimated. Table 3.5 shows the percentage of plant wax *n*-alkanes in the air particulate samples. The percentage concentrations of plant wax *n*-alkanes to the total concentration of *n*-alkanes in the air particulate samples ranging from 33.4% to 68.6%. The percentage for most air particulate samples is quite high.

Table 3.5: Percentage of plant wax *n*-alkanes in air particulate samples.

Sample	Percentage of plant wax *n*-alkanes (%)
1	56.6
2	51.5
3	49.5
4	65.9
5	44.3
6	39.2
7	64.6
8	58.8
9	55.1
10	59.8
11	42.9
12	43.6
13	42.7
14	67.1
15	68.6
16	47.8
17	62.7
18	61.9
19	n.a
20	59.1
21	59.7
22	54.2
23	54.5
24	62.3
25	33.4
26	33.4

*n.a = not available

By combining all the *n*-alkanes diagnostic parameters, the result shows that the air particulate matter over the Straits of Malacca, South China Sea and Sulu-Sulawesi Seas were enriched by higher plant wax *n*-alkanes, with significant contribution from algae, phytoplankton and bacteria waxes. It also shows the contamination from petroleum combustion.

3.4 *n*-ALDEHYDES

3.4.1 *n*-Aldehydes sources

The occurrence of HMW *n*-aldehydes has rarely been reported in airborne particulate matter. *n*-C_{26}, *n*-C_{28} and *n*-C_{30} aldehydes have been documented by Wils *et al*. (1982) in urban aerosols. HMW aldehydes have also been described in coastal sediments as indicators of higher plant inputs (Cardoso and Chicarelli, 1983; Albaiges *et al*., 1985, Phral and Pinto, 1987). They have been determined in sugarcane waxes (Lamberton, 1965), in fruit cuticles, (Croteau and Fagerson, 1971) and in cuticular waxes from foliage and pollen of decidious trees (Phral and Pinto, 1987). Aldehydes may occur in the epicuticular waxes as a result of the reaction of O_3 on unsaturated hydrocarbons, especially those with carbon atoms numbered higher than 20 (Rogge *et al*., 1998)

The homologues with lower carbon atoms number (C_9 to C_{19}) may originate by oxidation of alkanes and/or microbial sources or mixed anthropogenic processes (Stephanou, 1989). Often, the similarities of the chain length between natural occurring *n*-aldehydes and *n*-alkanols have led to the hypothesis that *n*-aldehydes represent the intermediates in the biosynthesis of alcohols from alkanes (Kolattukudy, *et al*., 1976). Low abundance of *n*-aldehydes in the environmental samples compared to *n*-alkanes also led researchers to suggest that the *n*-aldehydes are directly decarbonylated to *n*-alkanes during the process of biosynthesis.

3.4.2 *n*-Aldehydes characterizations

n-Aldehyde is an organic compound containing a terminal carbonyl group. This functional group, which consists of a carbon atom which is bonded to hydrogen atom and double bonded to and oxygen atom, is called the aldehyde group. The aldehyde group is also called the formyl or methanoyl group.

n-Aldehyde were characterized on *m/z* 82 fragmentogram (Figure 3.4). They were quantified using *n*-hexadecanal, *n*-octadecanal, *n*-eicosanal and *n*-tetracosanal. The aldehyde series detected in this research comprises of C_8 to C_{34}. Concentrations of *n*-aldehydes in air particulate samples vary from 0.001 ng/m^3 to 2.740 ng/m^3 (Table 3.6). This wide range of concentration happened because of not all C_8 to C_{34} *n*-aldehyde was detected in all air particulate samples.

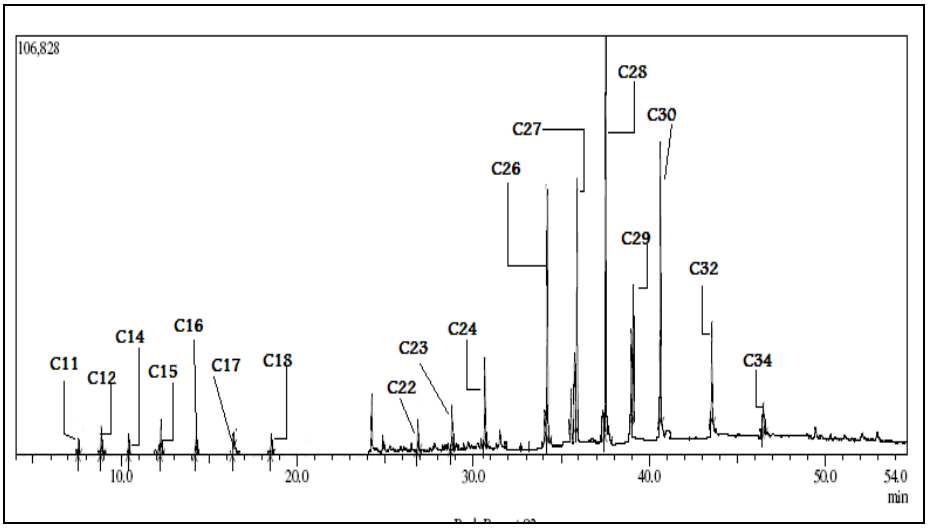

Figure 3.4: *m/z* 82 fragmentogram for the air particulate sample (S1).

Table 3.6: Total *n*-aldehydes concentrations for air particulate samples.

Sample	Conc. of *n*-aldehydes (ng/m^3)
1	0.689
2	n.d
3	0.001
4	0.980
5	0.286
6	0.668
7	0.751
8	2.740
9	2.200
10	2.000
11	1.620
12	2.510
13	0.793
14	2.260
15	1.140
16	n.d
17	0.662
18	n.d
19	1.840
20	0.338
21	1.690
22	0.001
23	1.000
24	1.680
25	0.726
26	0.572

*n.d = not detected

The CPI values for this homologous series were calculated using equation 3.4 (Page 24, section 3.2.1). Table 3.7 shows the CPI values of *n*-aldehydes in air particulate samples range from 0.4 to 5.6. It was not as high as expected for biogenic compounds. If we consider the range of C_{20}-C_{32}, these values were higher, indicating more biogenic input.

Table 3.7: CPI values of *n*-aldehydes for air particulate samples.

Sample	CPI value of *n*-aldehydes
1	0.4
2	n.a
3	n.a
4	n.a
5	n.a
6	0.7
7	5.6
8	1.9
9	1.0
10	1.0
11	3.0
12	1.2
13	n.a
14	n.a
15	n.a
16	n.a
17	n.a
18	n.a
19	n.a
20	n.a
21	2.2
22	n.a
23	n.a
24	2.2
25	n.a
26	n.a

*n.a = not available

Average chain length (ACL) values of *n*-aldehydes in all particulate samples are in the wide range of 26.7 to 29.5 (Table 3.8). These high ACL values indicate the greater contribution of terrestrial plant wax. Figure 3.5 shows the distribution of *n*-aldehydes in the air particulate samples. The *n*-aldehydes in the samples were dominated by *n*-C_{14} and *n*-C_{15}. Low carbon number *n*-aldehydes for C_{max} in the samples indicate the contribution from marine organisms.

Table 3.8: ACL values of *n*-aldehydes for air particulate samples.

Sample	ACL for *n*-aldehydes
1	26.7
2	n.a
3	n.a
4	27.6
5	n.a
6	n.a
7	n.a
8	28.1
9	27.9
10	n.a
11	n.a
12	n.a
13	n.a
14	29.2
15	29.5
16	n.a
17	n.a
18	n.a
19	n.a
20	n.a
21	n.a
22	28.0
23	n.a
24	n.a
25	n.a
26	n.a

*n.a = not available

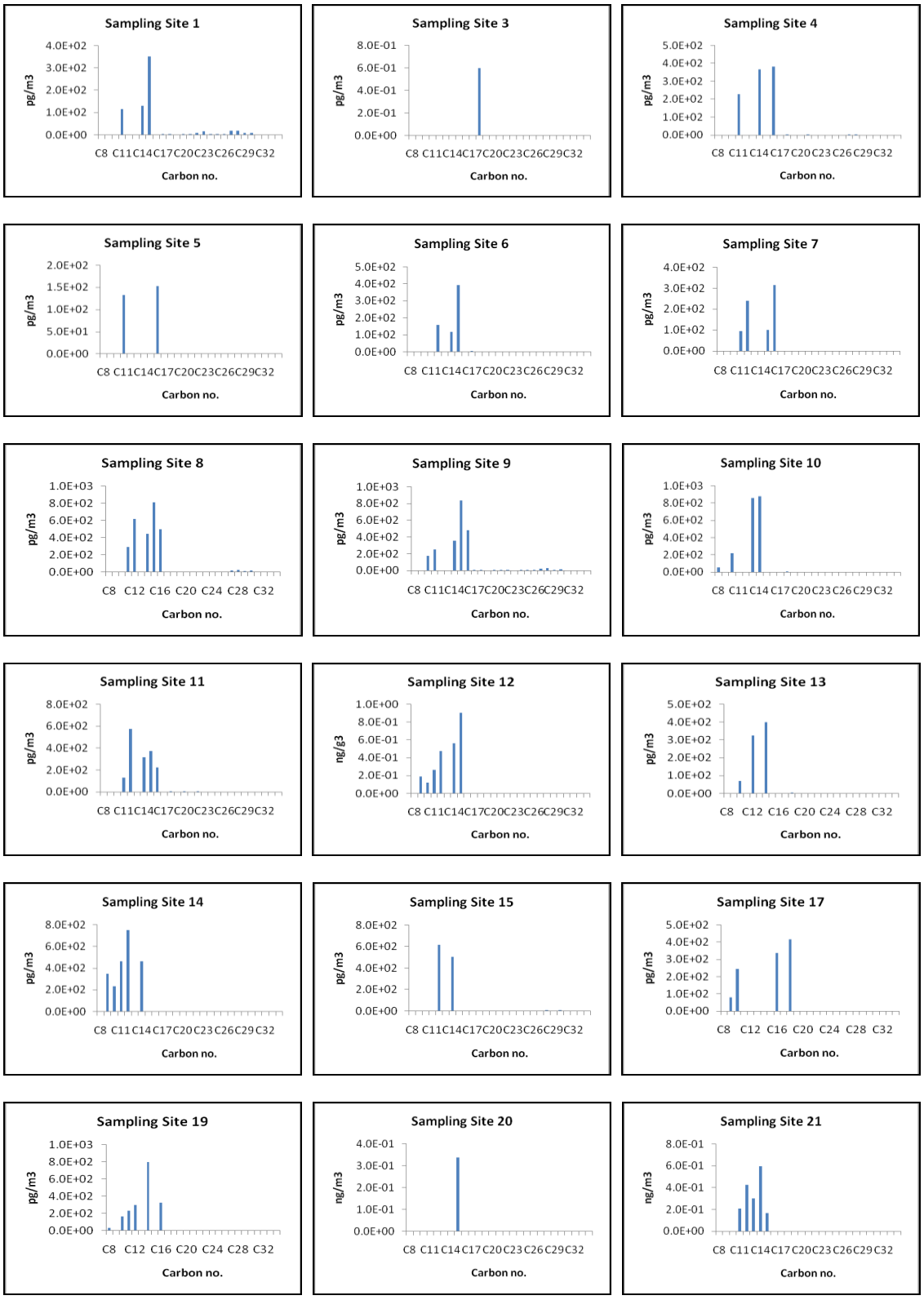

Figure 3.5: Distribution of *n*-aldehydes concentration in air particulate sample (Distribution for sampling site 2, 16 and 18 are not available).

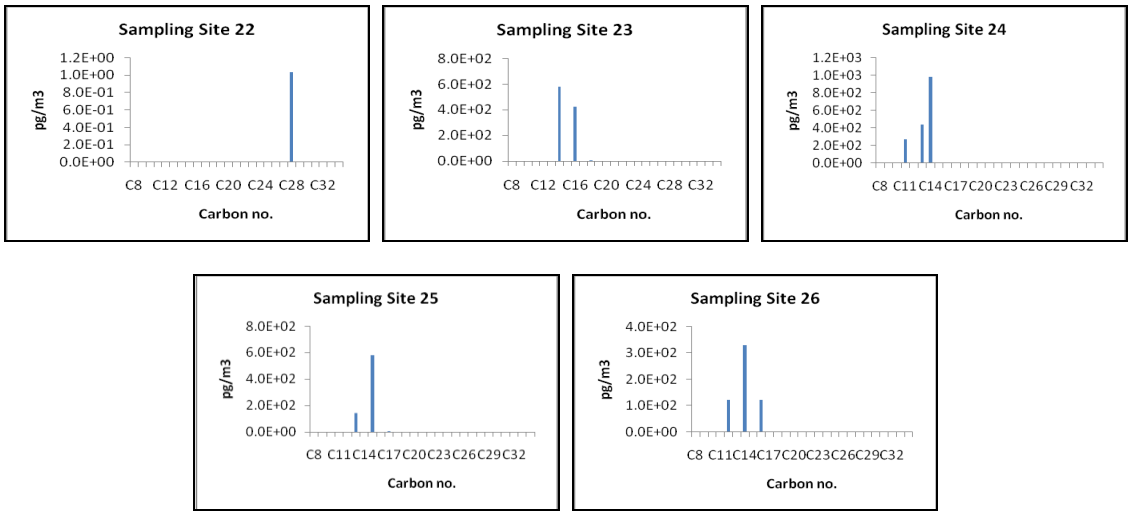

Figure 3.5(cont.): Distribution of *n*-aldehydes concentration in air particulate sample (Distribution for sampling site 2, 16 and 18 are not available).

LMW/HMW ratio of *n*-aldehydes (Table 3.9) are in the range of 5.29 to 79.50. High LMW/HMW ratio value suggested the higher contribution from low carbon number *n*-aldehydes. High LMW/HMW ratio in Sample 14 might comes from oxidation of alkanes from terrestrial plant wax, as the location of the sampling site is near to the land.

From this study, we can concluded that the *n*-aldehydes in air particulate matter may originate by oxidation of alkanes and/or microbial sources with a slight contribution of terrestrial plant.

Table 3.9: LMW/HMW ratio of *n*-aldehydes for air particulate samples.

Sample	LMW/HMW for *n*-aldehydes
1	5.29
2	n.a
3	n.a
4	n.a
5	n.a
6	n.a
7	n.a
8	21.90
9	17.40
10	n.a
11	n.a
12	n.a
13	n.a
14	79.50
15	22.60
16	n.a
17	n.a
18	n.a
19	n.a
20	n.a
21	n.a
22	n.a
23	n.a
24	n.a
25	n.a
26	n.a

*n.a = not available

3.5 *n*-ALKAN-2-ONES

3.5.1 *n*-Alkan-2-ones sources

Compared to other straight chain ketones, saturated *n*-alkan-2-ones are quite common and have been found in higher plant and phytoplankton biomass and a wide variety of depositional environments such as soils, peats, lacustrine and marine sediments, glacier ice, stalagmites and aerosols (Gao *et al*., 2008).

n-Alkan-2-ones usually occur in the form of homologous series ranging from C_{19} to C_{33}. Cranwell (1981) hypothesized that the resistance of various lipid classes with respect to degradation in anoxic environment were in the order of: *n*-alkanes > *n*-alkan-2-ones > sterols > *n*-alkanoic acids > *n*-alkanols > *n*-alkenoic acids. Some researchers proposed that microbial oxidation of *n*-alkanes and β-oxidation of fatty acids followed by decarboxylation could produce *n*-alkan-2-ones (Volkman *et al*., 1981; Lehtonen and Ketola, 1990). The *n*-ketones occurring in higher plants and phytoplankton are generally C_{23}-C_{33} mid-chain ketones with a high predominance of odd numbered carbon chain lengths maximizing at C_{25}, C_{27}, C_{29} or C_{31}.

The distribution of *n*-ketones in different geological samples typically showed similar distributions with a high predominance of odd-over-even carbon number homologues with maxima at C_{27} or C_{29} (Hernandez *et al*., 2001; Tuo and Li, 2005). Apart from natural sources, the anthropogenic discharge of cooking smoke, wood burning and automobile exhaust are also sources of *n*-alkan-2-ones.

3.5.2 *n*-Alkan-2-ones characterization

n-Alkan-2-ones were found in the second fraction of the column fractionation. Due to the lack of standards for *n*-alkan-2-ones, the whole homologous series of *n*-alkan-2ones were quantified based on the average response factor of tetradecan-2-one, nonadecan-2-one and hentriacontan-2-one. *n*-Alkan-2-ones in this study were characterized on *m/z* 59 fragmentogram (Figure 3.6). This method might underestimate some of the *n*-alkan-2-ones. Hernandez *et al.* (2001) classified the data obtained from this quantification method as semiquantitative data. Therefore, the data obtained from this study does not reflect the true concentrations of *n*-alkan-2-ones and only for comparison purposes to show the relative abundance of each *n*-alkan-2-one.

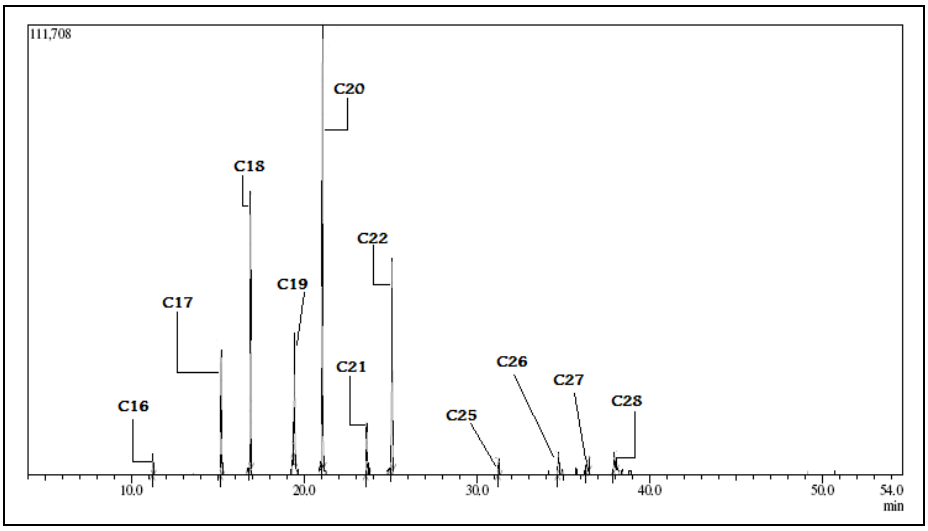

Figure 3.6: *m/z* 59 fragmentogram for the airborne particulate sample (S23).

The entire second fractions of the extracts contained the homologous series of *n*-alkan-2-ones ranging from C_9 to C_{35} with essentially an odd carbon number predominance. The *n*-alkan-2-ones concentrations on air particulate samples are in the range of 0.018 $\times 10^{-10}$ g/m^3 to 16.40 $\times 10^{-10}$ g/m^3 (Table 3.10). The lowest concentration is observed at sampling site 26 and the highest is at sampling site 9. Location of the sampling sites 9, which is close to the industrial area near Batam Island, might contribute to the abundance of long chain linear *n*-alkan-2-ones. For most of the sampling sites, the highest concentrations were observed for the long chain linear alkanones, characteristic of the waxy portion of the plant materials (Pio *et al*., 2001).

Table 3.10: Total *n*-alkan-2-ones concentration for air particulate samples.

Sample	Conc. of *n*-alkan-2-ones ($\times 10^{-10}$ g/m^3)
1	7.980
2	0.145
3	5.660
4	0.840
5	0.180
6	0.052
7	0.024
8	4.080
9	16.40
10	0.064
11	0.177
12	0.136
13	0.024
14	0.752
15	0.847
16	0.296
17	1.790
18	n.d
19	0.087
20	0.082
21	0.270
22	0.111
23	0.213
24	0.105
25	0.034
26	0.018

*n.d = not detected

CPI values for *n*-alkan-2-ones are in the range from 0.3 to 13.0 (Table 3.11). The highest CPI value is at sampling site 26, while the lowest is at sampling site 24. This result agree with the location of sampling site 26, which is nearer to the coastline, as *n*-alkan-2-ones are common in higher plant. Most of the CPI values for *n*-alkan-2-ones are high (>1). The results show strong odd over even carbon chain length predominance, indicating that the *n*-alkan-2-ones in the samples collected comes generally from higher plant wax.

Table 3.11: CPI values of *n*-alkan-2-ones for air particulate samples.

Sample	CPI value of *n*-alkan-2-ones
1	2.6
2	3.4
3	2.8
4	2.7
5	1.7
6	7.6
7	2.7
8	2.3
9	3.0
10	n.a
11	3.0
12	3.0
13	n.a
14	4.9
15	11.9
16	3.0
17	3.2
18	n.a
19	1.8
20	3.5
21	4.1
22	n.a
23	0.7
24	0.3
25	2.4
26	13.0

*n.a = not available

The average chain length (ACL) is a parameter that can be used to identify *n*-alkyl lipids from different vegetation. (Ternois *et al*., 2001; Boot *et al*., 2006; Jeng, 2006). Vegetation types are the main influence on chain length of terrigenous leaf lipids. For example, leaf lipids derived from grassland may have longer chain lengths on average than leaf lipids from plant in the forests (Cranwell, 1973). The *n*-alkan-2-one ACL data varied in the wide range of 27.0 to 30.5 (Table 3.12), indicating that the *n*-alkan-2-ones in air particulate matter collected may be from few different sources.

Table 3.12: ACL value of *n*-alkan-2-ones for air particulate samples.

Sample	ACL for *n*-alkan-2-ones
1	30.2
2	30.4
3	30.2
4	30.0
5	28.1
6	27.7
7	27.0
8	30.8
9	30.2
10	n.a
11	28.4
12	28.2
13	n.a
14	29.8
15	30.5
16	29.1
17	30.0
18	n.a
19	27.3
20	29.2
21	28.6
22	28.7
23	27.4
24	27.2
25	n.a
26	n.a

*n.a = not available

The distribution graphs (Figure 3.7) show in most samples, the concentration of *n*-alkan-2-ones are higher at carbon number C_{27} to C_{33}. The dominant peak occurred at C_{31} and C_{27} for eleven sampling sites, and at C_{14} at C_{16} for six sampling sites. This proves that the *n*-alkan-2-ones at these sampling sites comes from plant waxes as the long chain *n*-alkan-2-ones are typically found in the waxy portion of the plant materials.

The homologous < C_{20} however, are believed to be formed from anthropogenic activities, atmospheric oxidative processes, or microbial degradation of other compounds (Simoneit *et al.*, 1990b; Stephanou and Stratigakis, 1993).

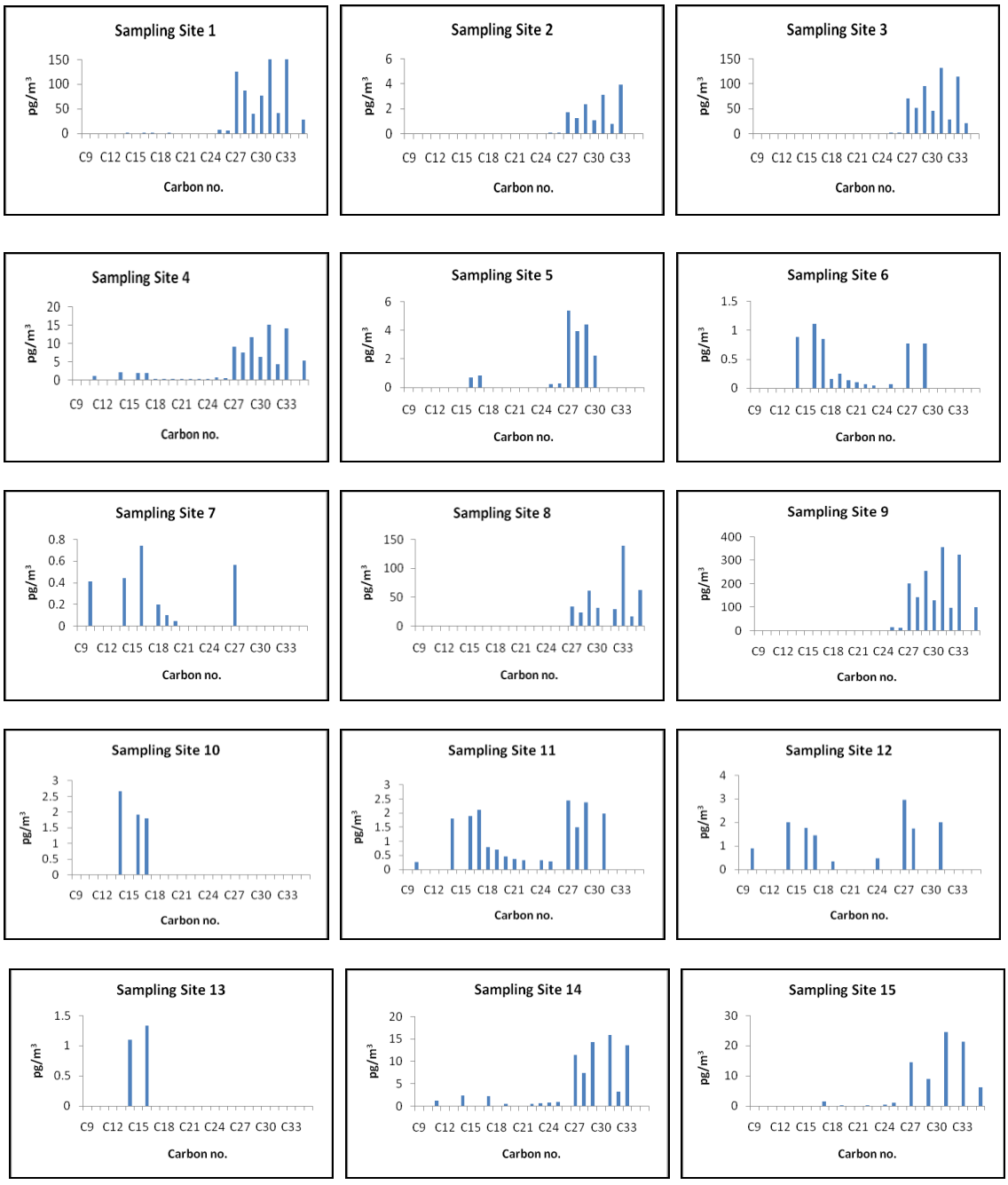

Figure 3.7: Distribution of *n*-alkan-2-ones concentration in air particulate sample (Distribution for sampling site 18 is not available).

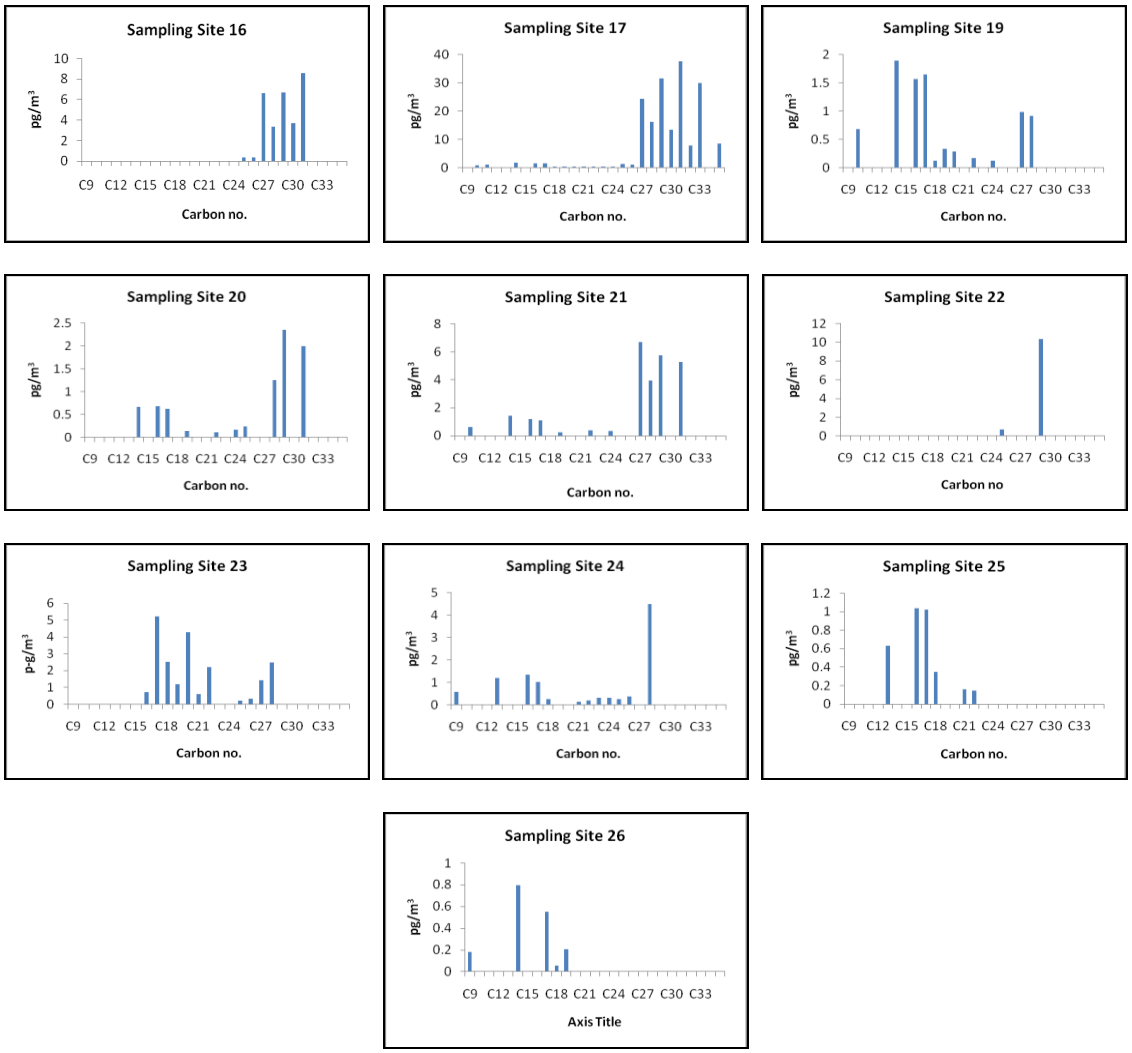

Figure 3.7(cont.): Distribution of *n*-alkan-2-ones concentration in air particulate sample (Distribution for sampling site 18 is not available).

LMW/ HMW ratios were mostly very low, no greater than 0.5 (Table 3.13), showing that the homologous with relatively longer chains are predominat members of the *n*-alkan-2-ones. However, at sampling site 25, the value of LMW/HMW is very high, indicating the greater contribution of short chain *n*-alkan-2-ones. This might due to the anthropogenic activities, oxidative processes or microbial degradation that occurs in that area.

Based on all the evidences, although there is no doubt that the majority of *n*-alkan-2-ones detected in air pariculate samples are from terrestrial higher plants, there is likely a sizeable portion of *n*-alkan-2-ones, both LMW and HMW, derived from anthropogenic input and/or degradation products of other lipids.

Table 3.13: LMW/HMW ratio of *n*-alkan-2-ones for air particulate samples.

Sample	LMW/HMW for *n*-akan-2-ones
1	0.01
2	0.01
3	n.a
4	0.14
5	0.09
6	2.04
7	2.43
8	0.02
9	0.01
10	n.a
11	0.88
12	0.78
13	n.a
14	0.09
15	0.03
16	n.a
17	0.04
18	n.a
19	2.67
20	0.35
21	0.18
22	n.a
23	2.17
24	0.46
25	17.63
26	n.a

*n.a = not available

3.6 *n*-ALKAN-1-OLS

3.6.1 *n*-Alkan-1-ols sources

n-Alkanols or fatty alcohols consist of a hydrocarbon chain and a hydroxyl group. In coastal environments, *n*-alkan-1-ols from fresh leaf waxes exhibit a pronounced even-ever-odd carbon number predominance of longer chain components, which mainly comprise the C_{20} to C_{34} homologues (Baker, 1982; Bianchi, 1995). Pancost *et al*. (2002) found that the *n*-alkanols in modern plants maximize at C_{24}, C_{26} or C_{28} homologue for the coarse root, leaves and stem.

Shorter chain *n*-alkanols are considered to originate from aquatic organisms such as bacteria or plankton (Ogura *et al*., 1990; Rielly *et al*., 1991). However, it has been argued that shorter chain *n*-alkanols are not accurate indicators of biotic sources due to their ubiquitous nature (Meyers *et al*., 1984).

3.6.2 *n*-Alkan-1-ols characterizations

n-Alkan-1-ols were found in fraction 3 and were quantified using *n*-hexadecan-1-ol, *n*-octadecan-1-ol, *n*-eicosan-1-ol, *n*-tetracosan-1-ol and *n*-heptacosan-1-ol. In this study, quantification was based on *m/z* 103 (Figure 3.8).

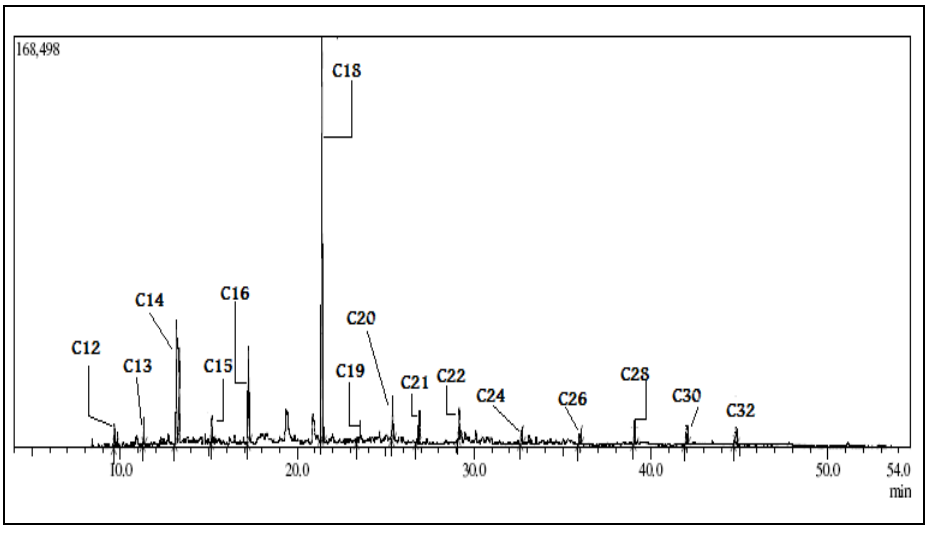

Figure 3.8: *m/z* 103 fragmentogram for the airborne particulate sample (S13).

The carbon chain length for detected *n*-alkanols series ranged from C_{10}-C_{34}. The concentrations vary from 0.107 ng/m^3 to 24.25 ng/m^3 (Table 3.14). The highest concentration is at sampling site 1 and the lowest is at sampling site 22. Low concentrations are likely due to the lack or limited contact with land. *n*-Alkanols is by far, the most abundant compound class determined among the neutral oxygenated lipids.

Table 3.14: Total *n*-alkan-1-ols concentration for air particulate samples.

Sample	Conc. of *n*-alkan-1-ols (ng/m^3)
1	24.25
2	0.791
3	1.905
4	1.963
5	1.240
6	0.829
7	1.228
8	17.95
9	13.07
10	2.191
11	0.282
12	0.531
13	0.315
14	1.931
15	3.632
16	3.933
17	1.497
18	1.519
19	0.162
20	0.862
21	1.653
22	0.107
23	1.459
24	1.728
25	0.299
26	0.167

The CPI values of *n*-alkan-1-ols are in the range of 0.6 to 11.3 (Table 3.15). The highest CPI value is observed at sampling site 10; the lowest is at sampling site 11. This might due to the location of both sampling sites. Sampling site 10 is nearer to the land,

while sampling site 11 is deeper into the open ocean. CPI values for most of the sampling sites are high (CPI >2). High CPI values show the strong even to odd carbon number predominance, suggesting that *n*-alkan-1-ols in these samples are mainly from fresh biogenic sources. Low CPI value at sampling site 11 shows a greater contribution from shorter chain *n*-alkan-1-ols, might be derived from bacteria and plankton.

Table 3.15: CPI values of *n*-alkan-1-ols for air particulate samples.

Sample	CPI value of *n*-alkan-1-ols
1	1.8
2	10.5
3	n.a
4	2.7
5	1.9
6	1.3
7	1.2
8	4.5
9	3.4
10	11.3
11	0.6
12	9.3
13	6.7
14	4.2
15	3.2
16	2.9
17	2.8
18	3.8
19	3.3
20	3.6
21	3.6
22	n.a
23	4.0
24	6.8
25	5.0
26	3.1

*n.a = not available

The *n*-alkan-1-ol ACL data varied in the wide range of 24.3 to 29.5 (Table 3.16), which was wider than ACL data for *n*-alkan-2-ones. This may be attributable to either sources or preservation differences. ACL value for most samples is more than 29. Low ACL values indicate the higher contribution of low carbon number alcohols, which sources might be, comes from aquatic organisms such as bacteria and plankton.

Table 3.16: ACL values of *n*-alkan-1-ols for air particulate samples.

Sample	ACL for *n*-alkan-1-ols
1	29.1
2	28.9
3	28.9
4	28.8
5	29.0
6	29.2
7	28.9
8	28.9
9	28.4
10	28.6
11	n.a
12	28.7
13	29.5
14	29.4
15	29.2
16	29.1
17	29.0
18	29.4
19	29.6
20	29.1
21	29.1
22	29.3
23	29.1
24	29.5
25	29.0
26	24.3

*n.a = not available

Distribution of *n*-alkan-1-ols concentration in air particulate samples is shown in Figure 3.9. The distributions of *n*-alkanols were characterized by an even carbon predominance. Most of the distribution shows the C_{max} at carbon number 28. The presence of large amounts of C_{28} suggests higher plant waxes as the source of these aerosol lipids. Long-chain *n*-alkanols are typically found in the waxy portion of leaf surface materials from plant and trees (Rogge *et al*., 1998). Very strong even-to-odd predominance and the presence of major amount of C_{28} suggests higher plant waxes as the source of these aerosol lipids. The distributions obtained here are similar to those obtained in other areas such as the North Pacific (Gagosian *et al.*, 1981), many locations in the United States (Simoneit and Mazurek, 1982) rural sites of Australia (Simoneit *et al*., 1991b) and the open Western Mediterranean (Simo *et al.*, 1990). The presence of small amounts of the low molecular weight homologs in air particulate samples presumably refelecting marine derived inputs (Garrett, 1967).

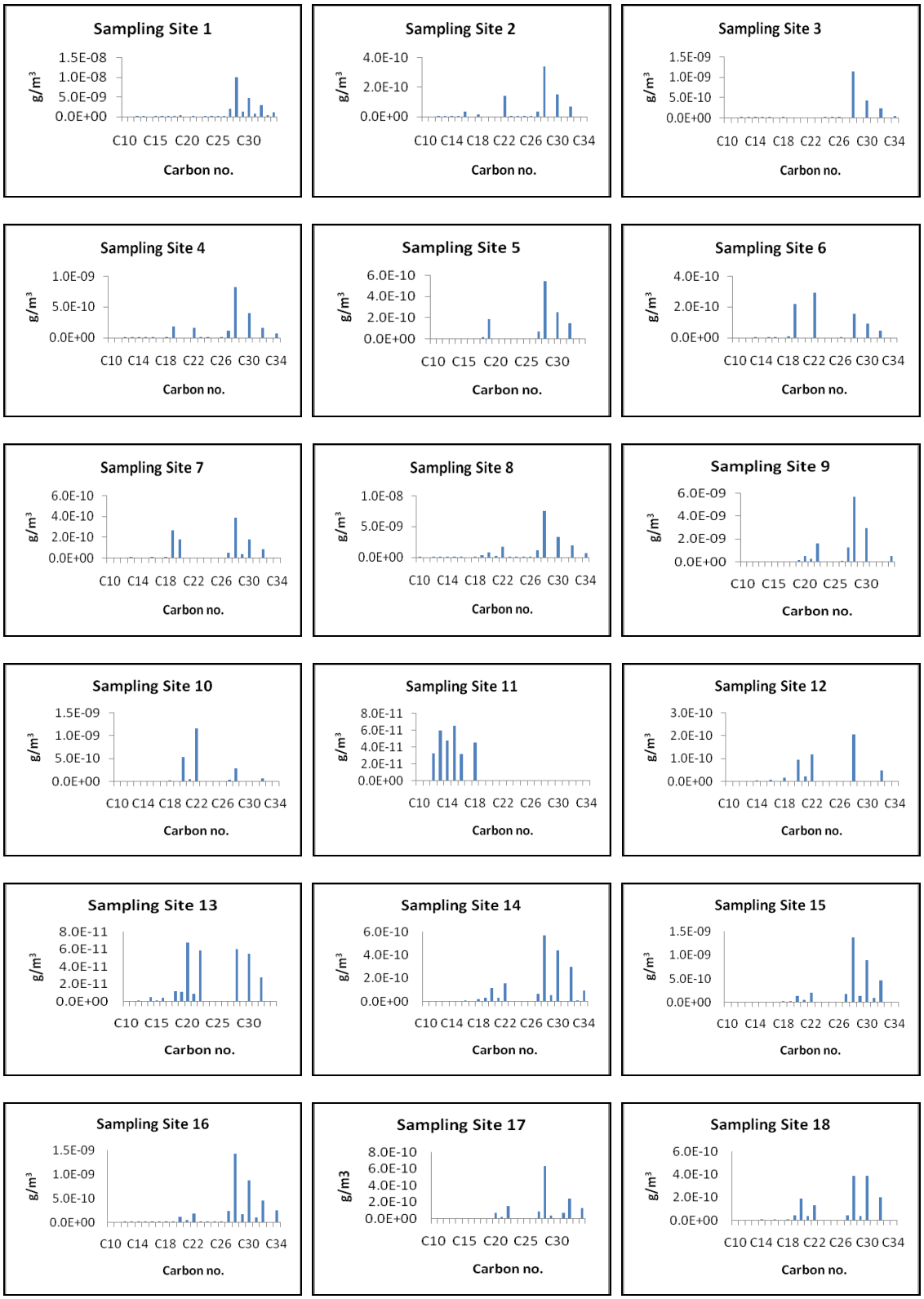

Figure 3.9: Distribution of *n*-alkan-1-ols concentration in air particulate sample.

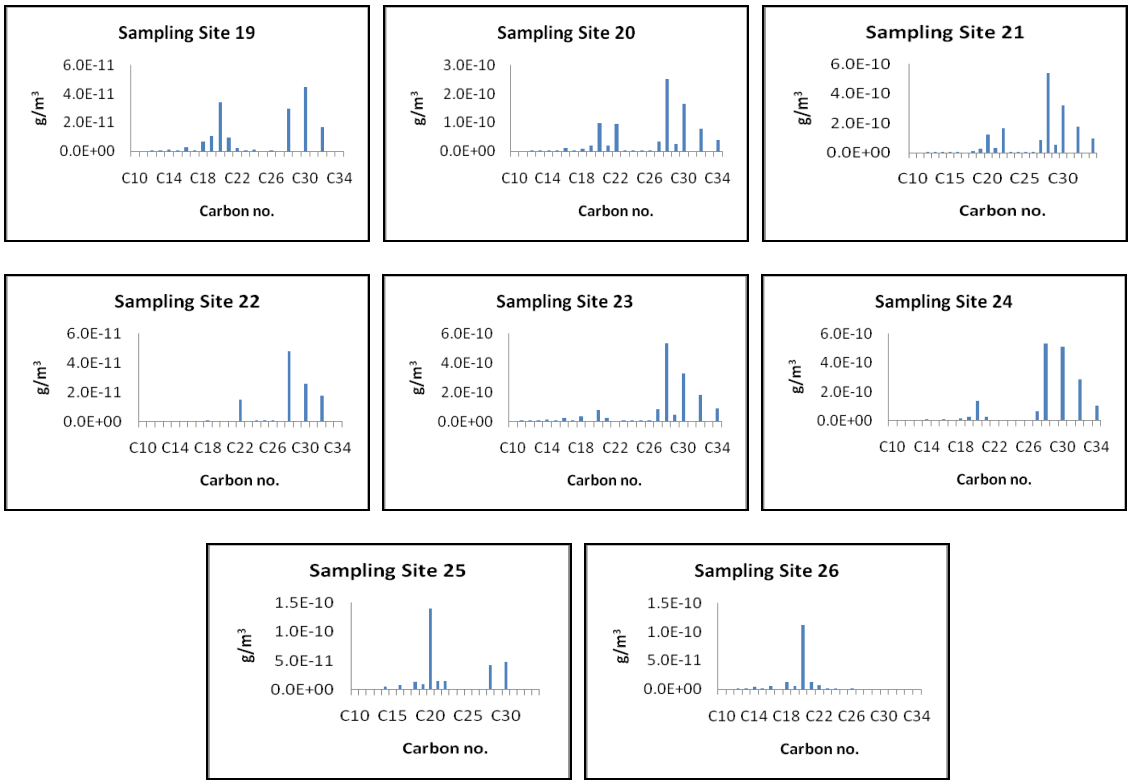

Figure 3.9(cont.): Distribution of *n*-alkan-1-ols concentration in air particulate sample.

The main assumption of using HPA index is that the ratio of primary fluxes of long-chain *n*-alkanes and *n*-alkanols is approximately constant over the total study area. The HPA value for air partculate samples studied were presented in Table 3.17. Most of sampling sites has the HPA value higher than 0.8. High HPA values indicate that the *n*-alkanols in the samples are not deeply degraded.

More recently, alcohol index (AI) was used to evaluate the relationship between *n*-alkanols and *n*-alkanes. AI value is presented in Table 3.18. Most AI values in the air particulate samples are low, indicating that the *n*-nonacosane is more abundance than *n*-hexacosanol. 2 of the sampling sites has an AI value of 1. This is due to the non-existence of *n*-nonacosane in the samples.

Table 3.17: HPA value for air particulate samples.

Sample	HPA value
1	0.80
2	0.62
3	0.46
4	0.95
5	0.95
6	0.96
7	0.90
8	0.93
9	0.88
10	0.89
11	n.a
12	0.81
13	1.00
14	0.91
15	0.94
16	0.94
17	0.87
18	0.87
19	1.00
20	0.88
21	0.67
22	0.51
23	0.87
24	0.83
25	0.90
26	0.18

*n.a = not available

Table 3.18: AI value for air particulate samples.

Sample	AI
1	0.13
2	0.04
3	0.03
4	0.37
5	1.00
6	1.00
7	0.35
8	0.28
9	0.20
10	0.21
11	n.a
12	1.00
13	1.00
14	0.23
15	0.34
16	1.00
17	0.18
18	0.19
19	1.00
20	0.20
21	0.06
22	0.13
23	0.21
24	0.13
25	0.21
26	0.17

*n.a = not available

The ratios of low molecular weight to high molecular weight of *n*-alkan-1-ols in air particulate samples are presented in Table 3.19. LMW/HMW ratio is in the range of 0.15 to 20.0. Low LMW/HMW ratio indicates the higher contribution of high molecular weight *n*-alkan-1-ols in the air particulate samples. High LMW/HMW value at sampling site 26 shows a greater contribution of low molecular weight *n*-alkan-1-ols ($<C_{21}$). It has been said that low molecular weight *n*-alkan-1-ols most probably comes from marine organisms and microorganisms. There are 2 sampling sites that has LMW/HMW

ratio greater than 1. In these particular samples, high concentrations of HMW *n*-alkanols were present. The homologous $>C_{20}$ are believed to be characteristic of vascular plants (Eglinton and Hamilton, 1967), while those $<C_{20}$ may originate from microbial or marine sources. (Simoneit and Mazurek, 1982; Weete, 1976).

Table 3.19: LMW/HMW ratio of *n*-alkan-1-ols for air particulate samples.

Sample	LMW/HMW for *n*-alkan-1-ols
1	0.04
2	0.07
3	0.02
4	0.12
5	0.19
6	0.41
7	0.64
8	0.09
9	0.08
10	0.39
11	n.a
12	0.40
13	0.54
14	0.14
15	0.08
16	0.06
17	0.09
18	0.25
19	0.69
20	0.25
21	0.15
22	n.a
23	0.15
24	0.16
25	1.81
26	20.0

*n.a = not available

Based on the results of all the parameters from the *n*-alkan-1-ols, we can conclude that the terrestrial higher plant waxes are the main contribution of *n*-alkan-1-ols in the air particulate samples. However, there are significant amount of marine origins in the few of the samples.

3.7 *n*-ALKAN-1-OIC ACIDS

3.7.1 *n*-Alkan-1-oic acids sources

As *n*-alkanoic acids are emitted from an important variety of sources in the environment, their presence cannot be reliably reconciled to a specific origin. Fatty acids from higher plant waxes show carbon number of more than C_{22} with a maximum at C_{24} or C_{26}, whereas those from algae and bacteria range between C_{12} and C_{20} with maximum at C_{16} (Eglinton and Calvin, 1967; Simoneit, 1978). Previous research has also shown that sewage discharge can bring fatty acids such as C_{16} and C_{18} to marine coastal areas and influence their original characteristics (Quemeneur and Marty, 1992).

Another source is represented by food preparation (Rogge *et al.*, 1991). The lower molecular weight *n*-alkanoic acids ($<C_{18}$) could also be found in emissions from petroleum-based sources, such as gasoline and diesel powered vehicle exhaust, or from distillate fuel oil, tire wear debris and road dust (Rogge *et al*., 1997).

3.7.2 *n*-Alkan-1-oic acids characterizations

The *n*-alkanoic acid consist of the carbonyl group (C=O) and hydroxyl (OH) group. A carboxylic acid can be generally represented by the formula $C_nH_{2n+1}COOH$. In this study, *n*-alkan-1-oic acids were quantified and characterized based on *m/z* 117 fragmentogam (Figure 3.10).

n-Alkan-1-oic acids with carbon number ranging from C_6 to C_{26} were recorded in the air particulate samples. *n*-Alkan-1-oic acid is not detected in all sampling site, as

shown in Table 3.20. The concentrations of *n*-alkan-1-oic acids detected are in the range of 0.003 ng/m^3 to 8.055 ng/m^3. The highest concentrations were observed from sampling site 1 while the lowest is at sampling site 13.

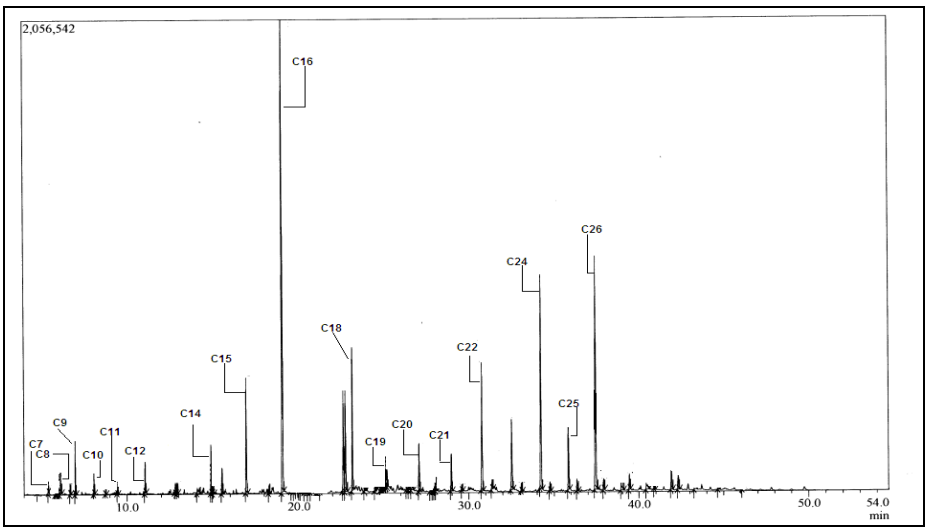

Figure 3.10: *m/z* 117 fragmentogam of air particulate sample (S9).

The carbon preference index (CPI) values detected are in the range of 1.3 to 30.2 (Table 3.21). The highest CPI value is at sampling site 4 while the lowest is at sampling site 18. Most of the sampling sites have high CPI value, clearly indicating that the *n*-alkan-1-oic acids in the samples are dominated by the components with even carbon numbers. This indicates a definite biogenic origin.

ACL values for *n*-alkan-1-oic acids were presented in Table 3.22. We can clearly see that the ACL values of *n*-alkan-1-oic acids are in the range of 24.0 to 25.6. ACL values for most of the samples are at C_{25}.

Table 3.20: Total *n*-alkan-1-oic acids concentration for air particulate samples.

Sample	Conc. of *n*-alkan-1-oic acids (ng/m^3)
1	8.055
2	0.606
3	3.881
4	0.047
5	0.085
6	0.041
7	0.037
8	0.372
9	1.219
10	0.082
11	n.d
12	0.014
13	0.003
14	0.008
15	0.008
16	0.098
17	0.033
18	0.039
19	n.d
20	0.031
21	0.237
22	0.012
23	0.175
24	0.035
25	0.015
26	0.013

*n.d = not detected

Table 3.21: CPI values of *n*-alkan-1-oic acids for air particulate samples.

Sample	CPI value of *n*-alkan-1-oic acids
1	10.1
2	4.1
3	16.6
4	30.2
5	17.9
6	13.1
7	6.5
8	8.4
9	11.1
10	6.1
11	n.a
12	2.0
13	n.a
14	18.9
15	n.a
16	n.a
17	n.a
18	1.3
19	n.a
20	4.9
21	8.8
22	n.a
23	6.0
24	n.a
25	13.6
26	10.6

*n.a =not available

Table 3.22: ACL values of *n*-alkan-1-oic acids for air particulate samples.

Sample	ACL for *n*-alkan-1-oic acids
1	25.5
2	25.6
3	25.6
4	25.6
5	25.4
6	n.a
7	n.a
8	25.6
9	25.6
10	25.4
11	n.a
12	n.a
13	n.a
14	n.a
15	n.a
16	25.4
17	25.4
18	n.a
19	n.a
20	n.a
21	25.3
22	n.a
23	25.3
24	n.a
25	24.00
26	n.a

*n.a = not available

n-Alkan-1-oic acids exhibited bimodal distributions (Figure 3.11) with maxima at C_{16} (for short chain homologous) and C_{26} (for long chain homologous). The homologous $<C_{20}$ are attributed to microbial sources or could even be contamination of petrogenic emissions from ship engine, while those $>C_{20}$ show a pronounced plant origin.

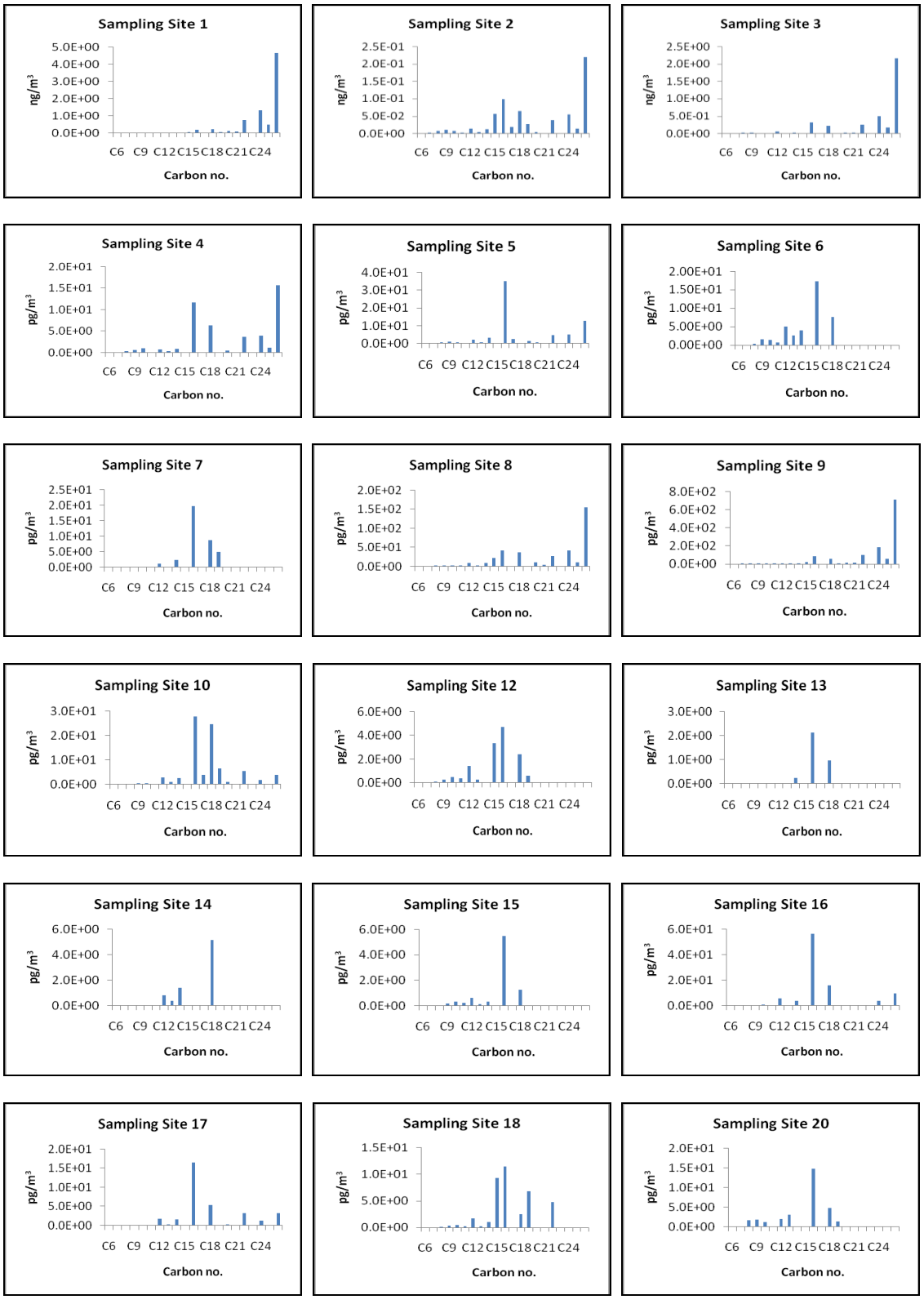

Figure 3.11: Distribution of *n*-alkan-1-oic acids concentration in air particulate sample (Distribution for sampling site 11 and 19 are not available).

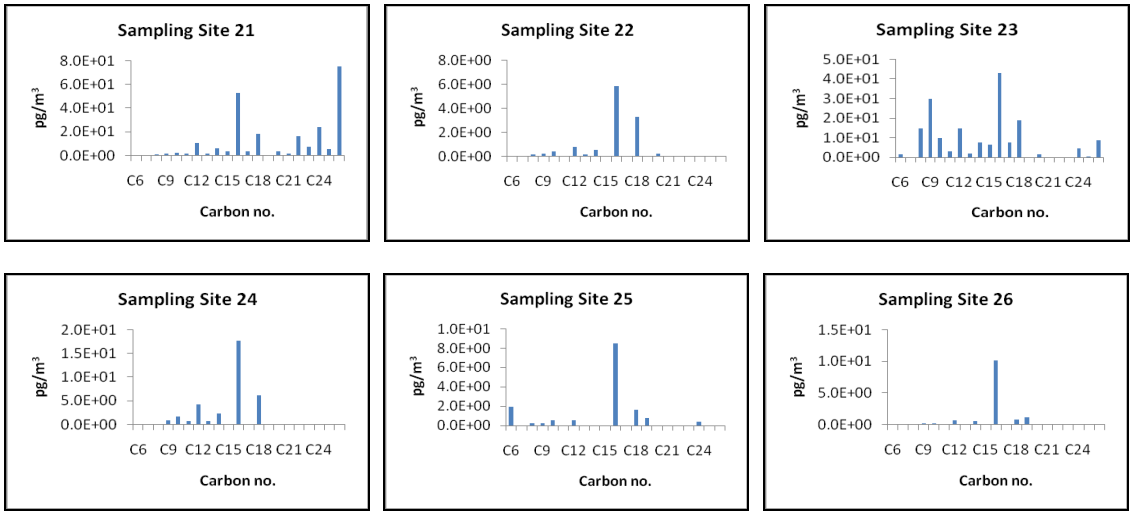

Figure 3.11(cont.): Distribution of *n*-alkan-1-oic acids concentration in air particulate sample (Distribution for sampling site 11 and 19 are not available).

LMW/HMW ratio of air particulate matter collected varies within a large range of 0.18 to 27.19 (Table 2.23), suggesting the contribution of *n*-alkan-1-oic acids from algae and bacteria is greater than that from higher plant waxes. The highest LMW/HMW ratio is at sampling site 25 while the lowest is at sampling site 9.

Based on all the results obtained for *n*-alkan-1-oic acids, it can be concluded that the *n*-alkan-1-oic acids fraction in the samples is dominated by the lower carbon homologous, which should mainly originate from marine sources, but also shows a terrestrial plant wax sources in lesser relative amounts.

Table 2.23: LMW/HMW ratio of *n*-alkan-1-oic acids for air particulate samples.

Sample	LMW/HMW for *n*-alkan-1-oic acids
1	0.09
2	0.87
3	0.20
4	0.80
5	2.50
6	n.a
7	n.a
8	0.50
9	0.18
10	6.00
11	n.a
12	n.a
13	n.a
14	n.a
15	n.a
16	5.44
17	3.07
18	6.58
19	n.a
20	n.a
21	0.67
22	n.a
23	6.23
24	n.a
25	27.19
26	n.a

*n.a = not available

4

CONCLUSION

Solvent extraction of airborne particulate matter yields hydrocarbons and hydrocarbon-like compounds such as *n*-alkanes, *n*-aldehydes, *n*-alkan-2-ones, *n*-alkan-1-ols and *n*-alkan-1-oic acids. The concentrations of the organic compounds are in the order of *n*-alkan-2-ones < *n*-alkanes < *n*-alkan-1-oic acids < *n*-aldehydes < *n*-alkan-1-ols.

The results of the extractable aliphatic organic matter show that the airborne particulate over the Straits of Malacca, South China Sea and Sulu-Sulawesi Seas were enriched with the higher plant wax. Terrestrial inputs are recognized at most of the sampling sites. Significant amount of short chain compounds, which are attributed to algae, phytoplankton, and/or bacteria are also present in the air particulate samples. This result agrees with the rich diversity of Straits of Malacca, South China Sea and Sulu-Sulawesi Seas.

Future perspective

Areas that deserved particular attention to improve the studies of airborne particulate matter over the Straits of Malacca, South China Sea and Sulu Sulawesi Seas are listed below:

- Determination of 6, 10, 14-ketones (trimethylpentadecan-2-one) in the air particulate samples. This compound has been proposed as the degradation products from phytol of chlorophyll.
- The trajectories and the wind speed of the study areas, as wind can carry the air particulate together with their contaminants from one place to another. If the wind speed and its trajectories can be determined, we can further investigate the origin of the compounds.

- Determination of levoglucosan and other sugars in the environmental samples, as sugars are common structural and storage compounds in both terrestrial and marine organisms and represent the major form of photosynthetically assimilated carbon in the biosphere.
- Determination of deicers used in the aviation industry, as Straits of Malacca, South China Sea and Sulu-Sulawesi Seas are the common pathway for planes to travel.